TECHNICAL REPORT PREPARED

FOR COIPAMINING
JUBA-SOUTH SUDAN

BY:
TERRACON S.R.L
Viale Giuseppe Mazzini , 40
CAP - 50132 – Firenze – Italia

COIPA
MINING COMPANY

COIPA
MINING COMPANY

PRESENCE IN SOUTH SUDAN SINCE YEARS

REPUBLIC OF SOUTH SUDAN

Report # 1

COIPA INTERNATIONAL
MINING COMPANY.

REMOTE SENSING TECHNIQUES FOR GOLD AND ASSOSSIATED MINERALS PROSPECTING

Exploration License EL 21

Concessions Exploration License
EL 21 DEIM ZUBIER AREA WESTERN
BAHER EL GHAZAL STATE
SOUTH SUDAN

Author:
Dr. Khalid Kheiralla
PhD Remote Sensing and Geological Modeling Team Leader

8 June 2018

Approved by:
Franco Caselli
Exploration Manager

COIPA INTERNATIONAL S.A.-BRANCH * Reg. N°:45728 *

Report # 1

COIPA INTERNATIONAL MINING COMPANY.

REMOTE SENSING TECHNIQUES FOR GOLD AND ASSOSSIATED MINERALS PROSPECTING

WAU CONCESSION AREA, BLOCK EL 21

WESTERN BAHER EL GHAZAL STATE, SOUTH SUDAN

BY: PD. DR. KHALID MUSTAFA KHEIRALLA

Contents

1. INTRODUCTION

The gold and associated minerals are common all over Wau region Western Bahr eL Ghazal State of the Sudan, from regional geological maps the Block EL 21 in Wau region is covered with loose and weakly sediments Mesozoic Cainozoic age sediments of greenstone. The study area is situated within the COIPA mining company concession area. The concession area is approximately L shape of land about 2478 km2 with its 77 km longer axis trending roughly east-west as viewed on the satellite image and location map in (Fig.1) and cover by NC_35_N_RAGA and NB_35_B_DEIM ZUBEIR-sheet 1:250 000. The project area nearest (eastern) side lie around 65 km distances from Al Radom National Park (Fig.1). However, the project area is mapped as shown in figure (1) and defined by the following coordinates in Table (1):

Table 1: The coordinates of the main vertices of the project area

Long.	Lat.	Corner
26.20000	8.10833	1
26.20000	7.78333	2
26.63333	7.78333	3
26.63333	7.61667	4
25.93333	7.61667	5
25.93333	8.10833	6

This report represents the preliminary findings of the geologic remote sensing study on COIPA mining company concession area, Western Bahr eL Ghazal State in northwestern part of South Sudan. The area under consideration is about 2478 km^2 approximately. Deim Zubeir, Sopo and Kuru are the main settlements within the block EL21. There is a motor truck which extends from Kuru eastwards till it crosses the Deim Zubeir town and northwestwards to Sopo. Wau, the headquarters for Western Bahr eL Ghazal State is about 155 km east the block EL 21. Wau is linked with Al Obeid by a railway line. Wau is also connected with Khartoum and Juba by aero-plane service, once a day. It has a proper hospital, a regular and post and telegraph, service and the market is well provided with food stuff, clothing materials and other commodities. The road from Wau is open during the dry season only and needs annual minor repairs after the rainy season, there is a they motor route, from Deim Zubeir and Kuru and , running north to Sopo, then to Raga. This is also a dry season route with numerous temporary timber bridges over the streams (Fig. 1).

The area is generally flat with a thick reddish laterite bodies, rising gradually and gently northeastwards until it reaches the Bahr el Ghazal swamps area running roughly northeast and demarcating the watershed between the Baher El Arab and White Nile basins. The block EL21 cover by low hills with strike mainly NE, this hills comprises J. Tagwa, J. Ungabongbo, J. Nimbi, J. Ungo and J. Kuru. The study area was covered with laterite bodies that are occasionally overlain by thin loose soil. The laterite bodies may exist in forms of sheets, ridges or as boulders. The physical characteristics of laterite vary from

reddish brown and massive when iron seems to light brown and rather friable with patches of white and yellow colour that often indicate bauxite. Although chemical analyses will show the relative amounts of Al and Fe defining presence of bauxite, observed physical appearances indicates the existence of packets of bauxite in the area.. A local watershed trends NE – SW following the orientation of the volcanosedimentary unit. The area is drained to Bahr eL Arab, by meandering water courses

Wau region has a savanna to tropical climate, with a dry period from November to May and rainy season from May to October, Average rainfall is 1000 mm. Temperatures are usually high through the year ranging from 18° to 25° in winter and average 43°C in May, June and July. The area is well forested with rather scrubby types of trees and shrubs, which include a for proportion carrying thorns. Larger trees, some apparently of good timber types, are sparsely distributed along the banks of River Chel and River Sopo, Adda and to a lesser extent along the minor channels. Tebaldi (Baobab) Trees are not present, but bamboos are widespread and in some places fairly thick liban trees (Euphorbia) are also widely distributed in some localities, grasses, largely burned off in the dry season are usually thick and grow about six feet high, tropical mango trees grown extensively on both eastern and western banks of River Chel in eastern and River Sopo western part of the concession area. The wildlife population found in the area Um Dik Dik, Pigs, Wolfs, Rabbits, Dear, Gazelle, Monkeys, Ibes and Nakar (mountain sheep). The area becomes impassable during this rainy season as the streams flow continuously and tremendous Stretches of land become swampy or at least very muddy.

The general altitude of the plain is range between 700-500 m above mean sea level, and it is dipping at very gentle slope to the north east toward the Bahr eL Arab Basin. Some protruding low hills or hill chains that hardly exceed 60 meters above the surrounding plains occasionally break the flatness monotony of the plain. These hills tend to form elongated NW-SE trending ridges mostly acting as water divides controlling the drainage dividing the study area waters to the northeast and southwest.

The streams are winding, narrow, shallow with gradual slope and wet to most part of the year, which are controlled by the general structure manifested in the fault system in upstream these wadis exhibit feather-like drainage system (Figs. 3 & 7). River Sopo, R. Chel, R. Biri, Khor Gannam, K. Gankur, R. Kuru, R. Reidie, and R. Mana are the dominant streams in the area; it flows northeast and east to join the Bahr eL Arab. Occasionally, the basement outcrops as isolated low relief hills, making the terrain undulating, with recent superficial deposits filling the dry stream valleys. The drainage system and the watersheds of the region are extracted from the SRTM data. Individual channels are determined by applying Arc Hydro flow routing algorithm and by the calculation of the upstream drainage area.

The regional high-density stream sediments geochemical surveys are essential first step of exploration and are based on the hydrographic (drainage) network. Drainage patterns conform to some degree to the regional slope of the terrain, and to its underlying geological structures. This involves assessment of the geo-morphological history of the area and the stage of development of the landscape dissection. Streams propagate themselves and developed tributaries by head ward erosion. They tend to follow the line so fleast resistance. Therefore, some drainage may change the old direction in the areas, which have

a frequent extensive heavy rainfall. The shapes of valleys in cross sections can be important criteria identifying underlying lithologies. Similarly, the drainage density can play an important discriminatory role. However, both are strongly affected by climate. Surprising, drainage density in an arid area on any particular rock type is usually greater than on developed under humid conditions.

The parts of R. Chel and R. Sopo upstream of Deim Zubeir area cease to flow as from October, but separate pools are left ill the main channels until probably the end of December. After that date, the pools dry out and the local people get their water by digging shallow pits (gammam) in the sands of the khor beds. Some shallow depressions, which exist away from the main streams, are able to retain small quantities of water for several months. There pools and traps are extremely valuable for the people who have to traverse this hinterland on foot during the dry season. Potable water supply is rather difficult; water is obtainable from the streams only during rainy season (June- October). In the dry season, water obtainable from shallow wells dug in the streambeds. In the study area markets, the government has established a water donkey for all year round water supply.

The study area is scarcely inhabited by number of Banda tribes, along the road link between Wau and Sopo and further south the inhabitants are the Fertit tribes, with no sharp tribal boundary between them and the Kreishandog, but the most of the areas uninhabited. Besides the original settlers, there are always newcomers of Denka, from across the Warap and Al-Buhyrat States. The main occupation of the Banda, who are always village dwellers, is agriculture; fattarita comprise the main crops, with limited sesame cultivation. On the other hand, the Fertit is herdsmen owing cattle in big number. These people are in constant migration between central and south Darfur, seeking good grazing places. When the raining season is over groups of them flock southward and cross the Rivers.

The study is based mainly on geological mapping using remotely sensed data and on digital image processing, visual interpretation and spectral and spatial analysis in GIS framework with fieldwork or ground truth checking. The main objective of the study is to create a geological map and delineate various structural aspects of the area in addition to pilot prospecting work to pin point the gold deposits and associated minerals, which could be related to mineralization zones.

The multi-spectral of Landsat 8 and ASTER images and beside the elevation data of SRTM (Shuttle Radar Topography Mission) are the main source of this study beside previous geological maps and reports.

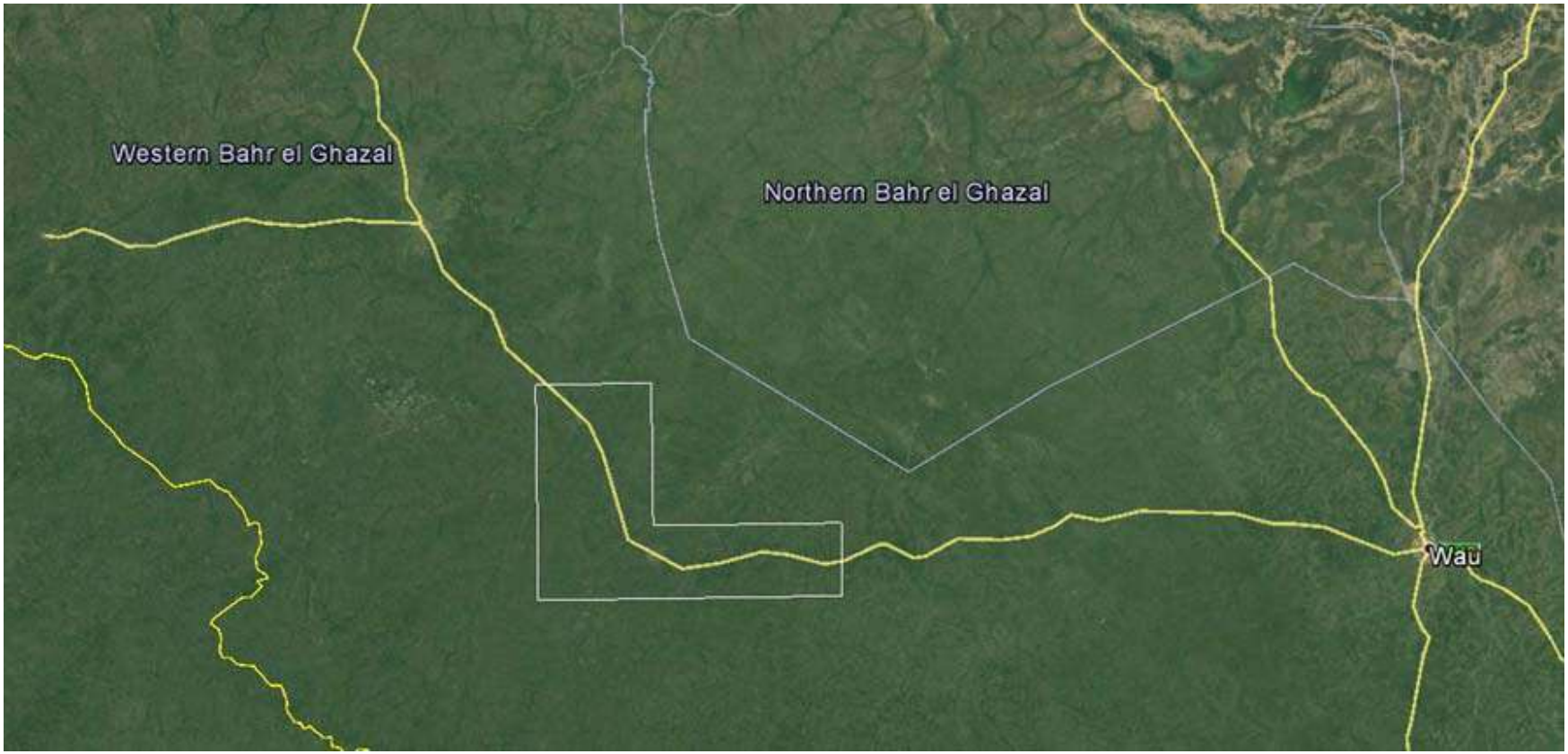
Western Bahr el Ghazal
Northern Bahr el Ghazal
Wau

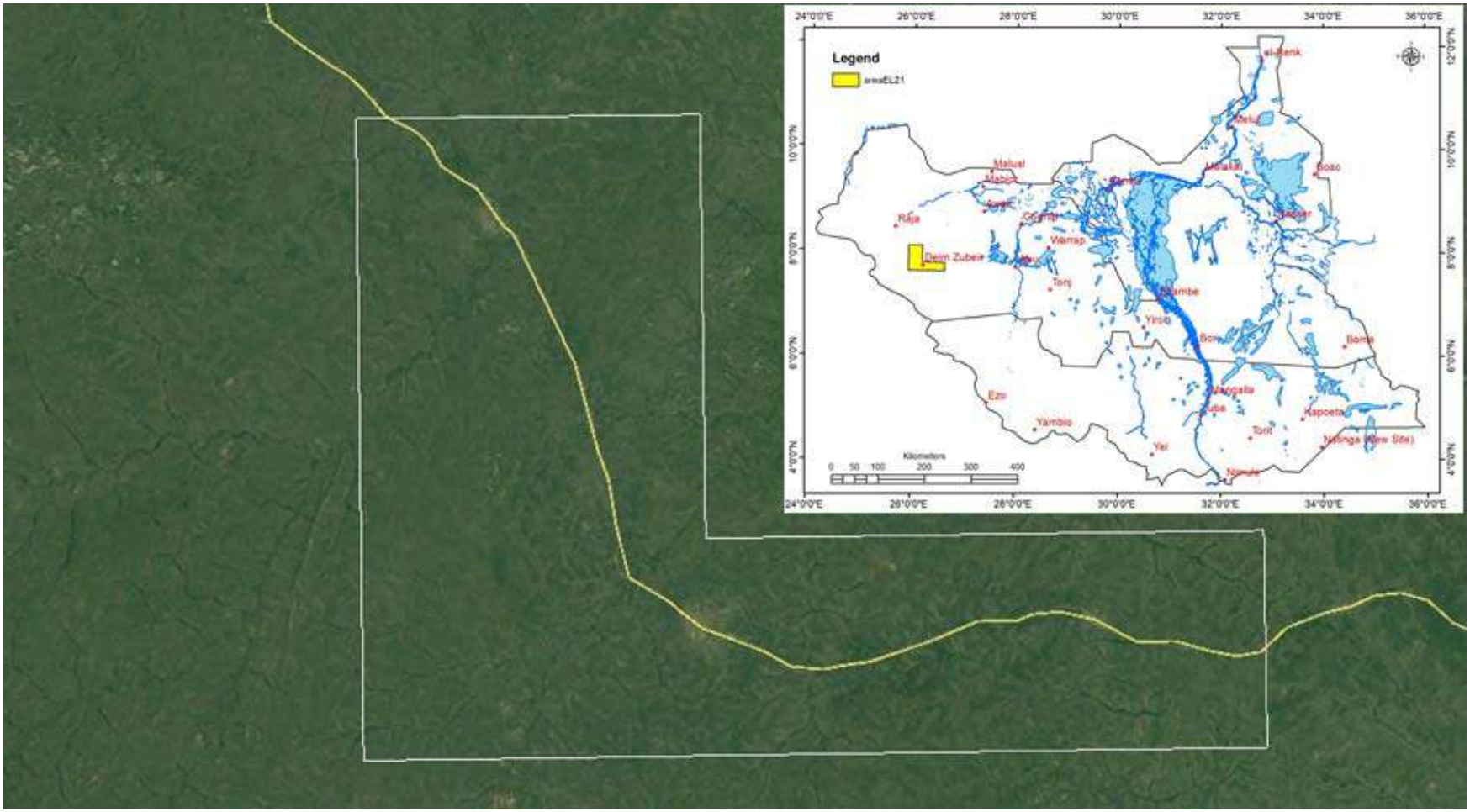

Fig. 1a. Location of the study area, a Google Earth's image cover the Coipa mining block EL21

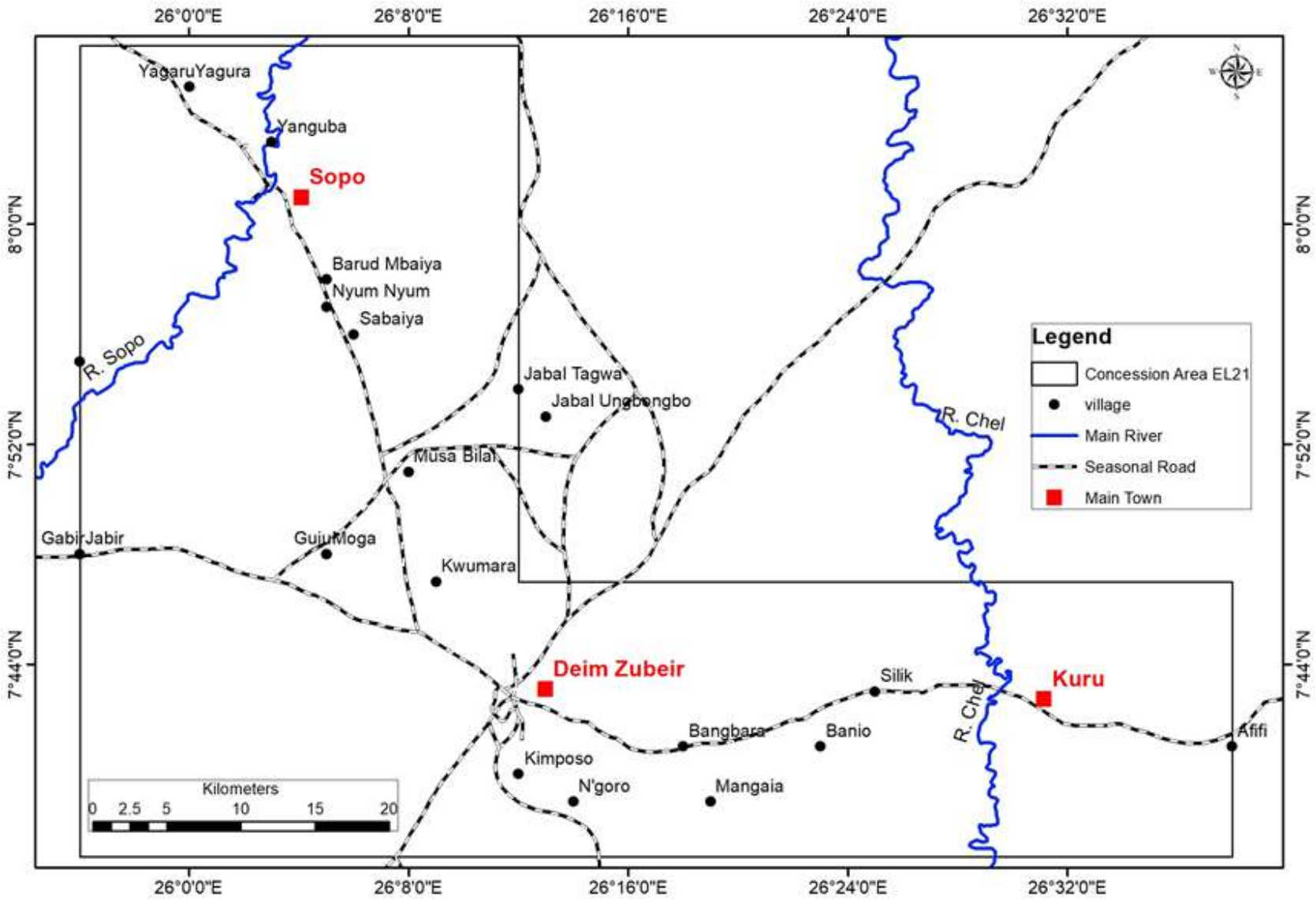

Fig. 1b. Settlement and infrastructure map of the study area

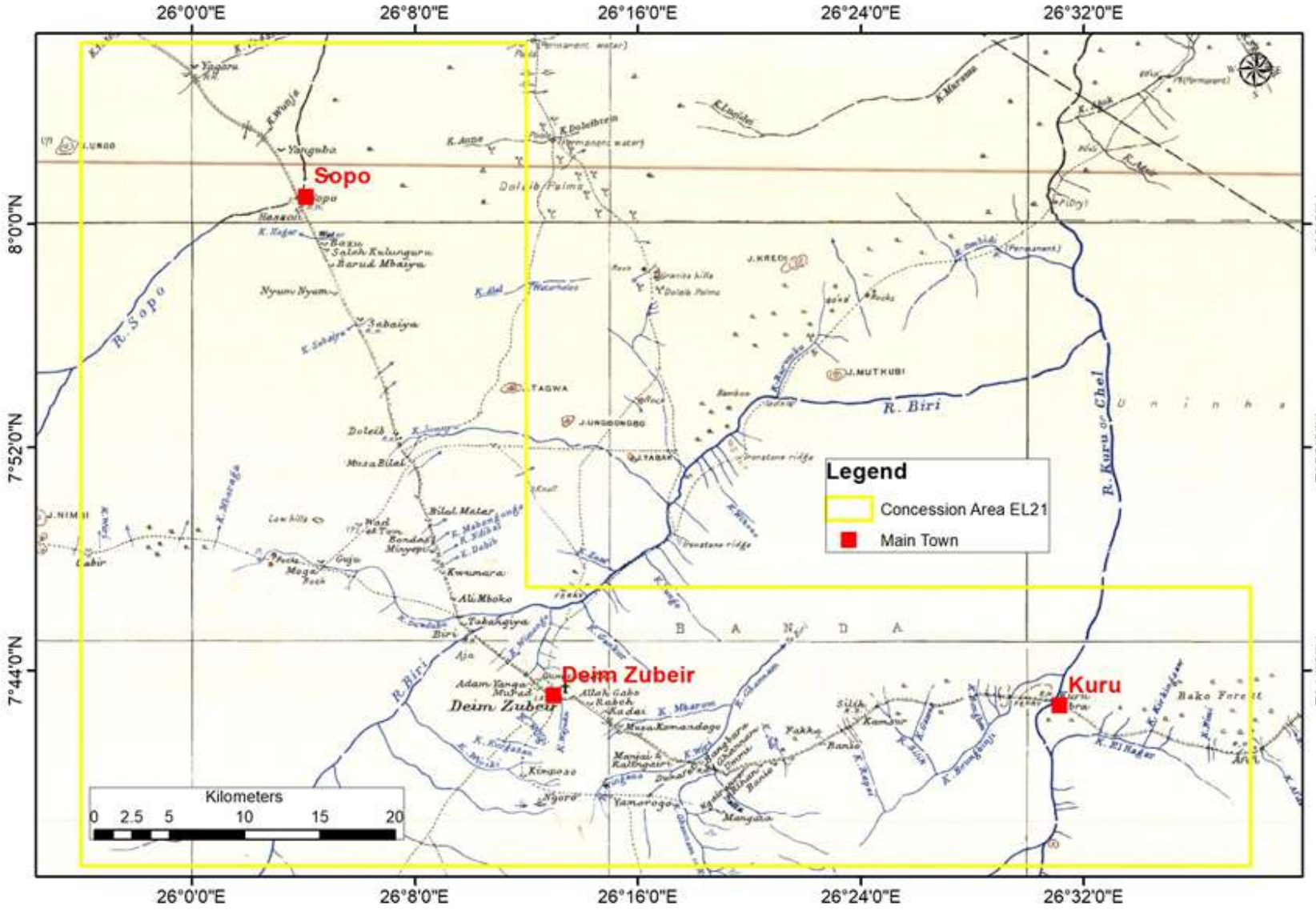

Fig. 1c. Topographic map the study area (cover by: NC_35_N_RAGA and NB_35_B_DEIM ZUBEIR-sheet 1:250 000)

2. REMOTE SENSING INVESTIGATION

The Wau area is not ideal for obtaining good, clear satellite images as it has a large number of cloud free days, and dense vegetation cover the images from both the Landsat and ASTER series of satellites were is difficult for interpretation. At the outset the data for one ASTER scene was purchased to cover the original area of interest (AOI), so far this image is being used to cover the revised AOI and their location and acquisition dates (the acquisition dates are 26/02/2006). The map also shows the area covered by four scene Landsat image (ETM+7 and L8 OLI) data which was downloaded free from the USGS GLOVIS website, the scene is Path 177-176 Row 54-55 acquired on 30th November 2013.

ASTER is the Advanced Space borne Thermal Emission and Reflection Radiometer; it was launched on the Terra satellite in 1999 as part of a joint mission between NASA and the Japanese government. The satellite carries three instruments for the ASTER mission and these acquire data in the VNIR (visible near infrared), SWIR (short-wave infrared) and the TIR (thermal infrared) parts of the electromagnetic spectrum. ASTER has a number of benefits over Landsat, mainly because it has 14 as opposed to 7 spectral channels and the near infra-red channels have 15 m pixel size as opposed to 30 m for Landsat. Using ASTER data, a wide range of band combinations and ratio images can be generated to assist in the location of iron and argillic alteration minerals which can be indicative of mineralised zones. A comparison of the two systems is presented in figure (2a).

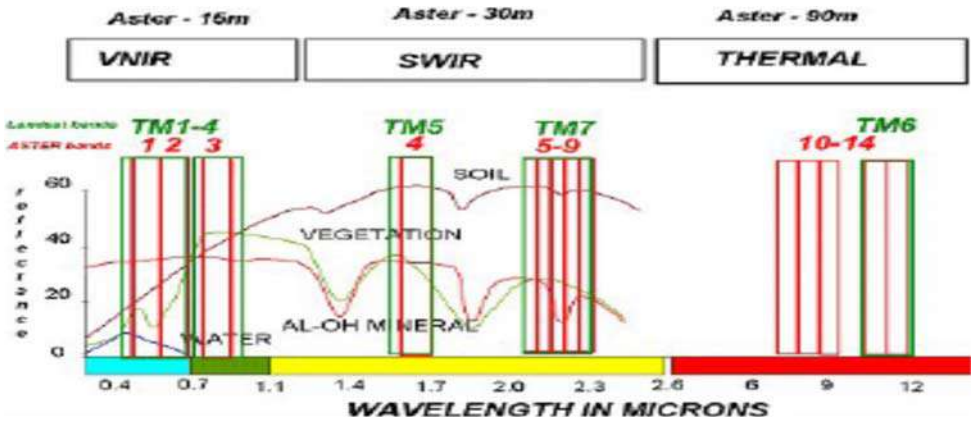

Fig. 2a. Comparison of the Spectral Range of ASTER and Landsat

The following remotely sensed data have been used in this study:

I. ASTER, Landsat 8, ETM+7 data, path 176 and 177, row 54 and 55, acquisition date 30th November 2013 and 30th November 2002 respectively, with 6 multispectral bands and panchromatic of spatial resolution 15 m and 30 m, respectively (Fig. 2b).
II. Digital Elevation Model data of SRTM (Shuttle Radar Topography Mission)

Whereas auxiliary data are:

III. Geological Map of the Sudan (GRAS, 2005).
IV. Robertson Research Map (GRAS, 1988).

All the raster data have been put in a GIS compatible format, the main aim of the digital image processing in the first stage is to produce enhance images suitable for visual interpretation of the geology and facilitate the discrimination of various lithological units and decipher the main structural elements of the area under consideration. All the raster data have been resampling into 15 m pixel size to achieve the required map scale of 1:75000.

Different algorithms have been utilized in this study in order to obtain different color composite images, which are used in visual interpretation and mapping the geological units and boundaries, such as:

- Haze correction for removal of atmosphere effect, which have been done on relative method.
- Linear stretch enhancement.
- Transformation algorithms to obtain new images, in this context the PCA transformation, Deccorrelation stretch and band ratio transformation have been applied.
- Fusion algorithms have been applied using the IHS transformation for the Linear stretched and Deccorrelated stretched image to enhance the spectral and spatial characteristics of these images.
- Unsupervised classifications have been applied to gain a preliminary idea about the geological boundaries and units.

Additional image processing using ASTER data included the creation of structural enhancement, lithological discrimination, advanced argillic alteration and gossan-alteration-host images. The ratios used are summarized in Table (1) below.

The following figures (3, 4, 5, 6 and 7) display various images used in the study:

Table 2: Processed Images Generated for Interpretation

IMAGE	BAND COMBINATION/ PROCESSING	FILE NAME
ASTER bands 3,2,1 as RGB	False colour 321 combination	Aster_0xx_B321 (0xx = scene ID)
Landsat Bands 7,5,2 & 8 combined as RGB & intensity	False colour 7528 combination	Landsat_ B7528
ASTER bands 7,4,2 as RGB (Structural enhancement)	False colour 742 combination	Aster_0xx_B742 (0xx = scene ID)
ASTER Sultan Ratio (Lithologic discrimination)	Ratio: (4/7 red), (4/1 green) and [(5/6)*(4/3) blue]	Sultan_Disc_Ratio_0xx (0xx = scene ID)
ASTER Sabins Ratio (Lithologic discrimination)	Ratio: (3/1 red), (5/7 green) and (3/5 blue)	Sabin_Disc_Ratio_0xx (0xx = scene ID)
ASTER Gossan/Alteration/Host Ratio	Ratio: (4/2 red goss), (4/5 green alt) and (5/6 blue-host)	GAH_Ratio_0xx (0xx = scene ID)
AlOH minerals/advanced argillic alteration	Ratio: (5/6 red goss), (7/6 green alt) and (7/5 blue-host)	AdvArg_Ratio_0xx (0xx = scene ID)

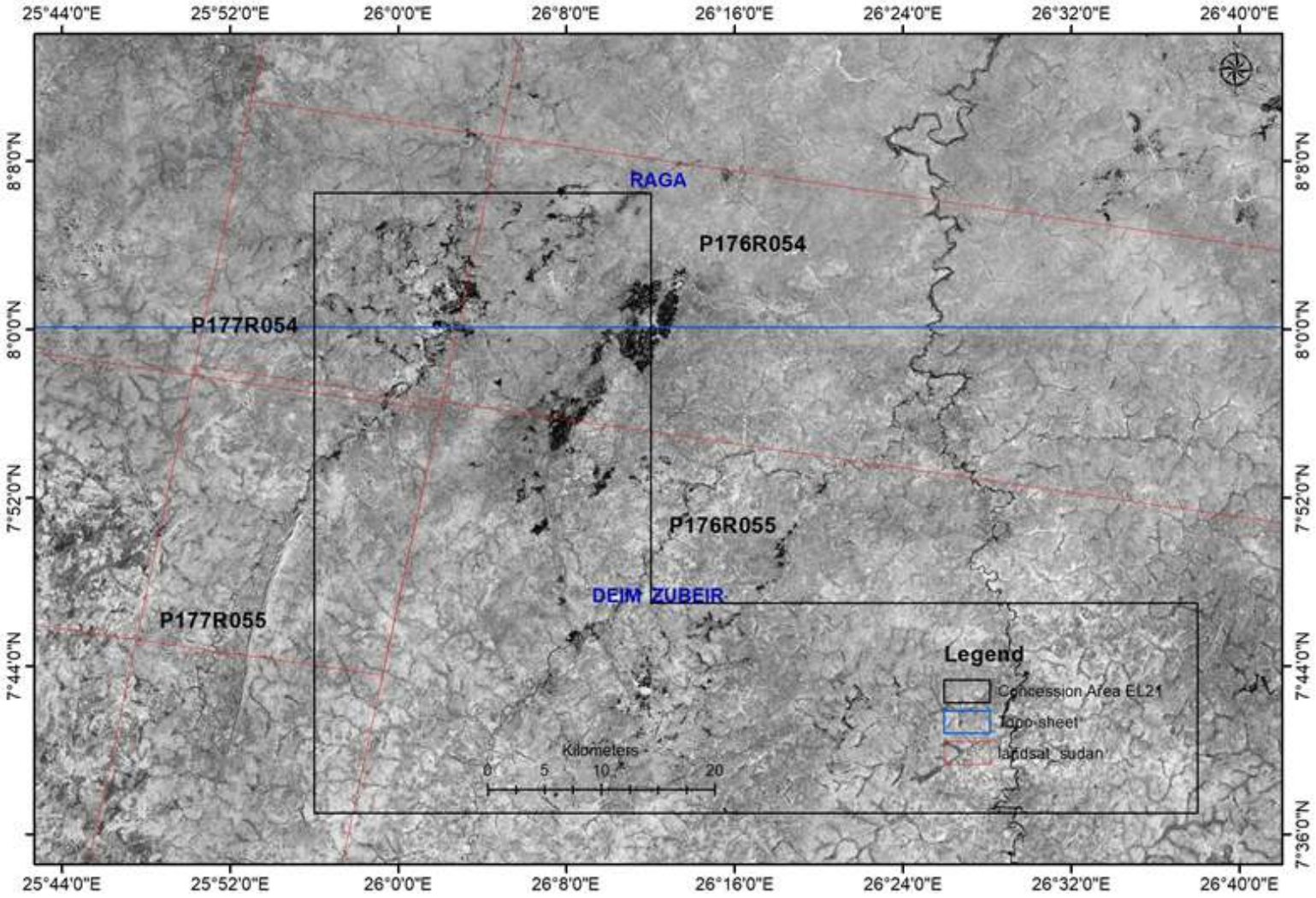

Fig. 2b. Location of the concession area cover by topo-sheet and Landsat 8 scenes

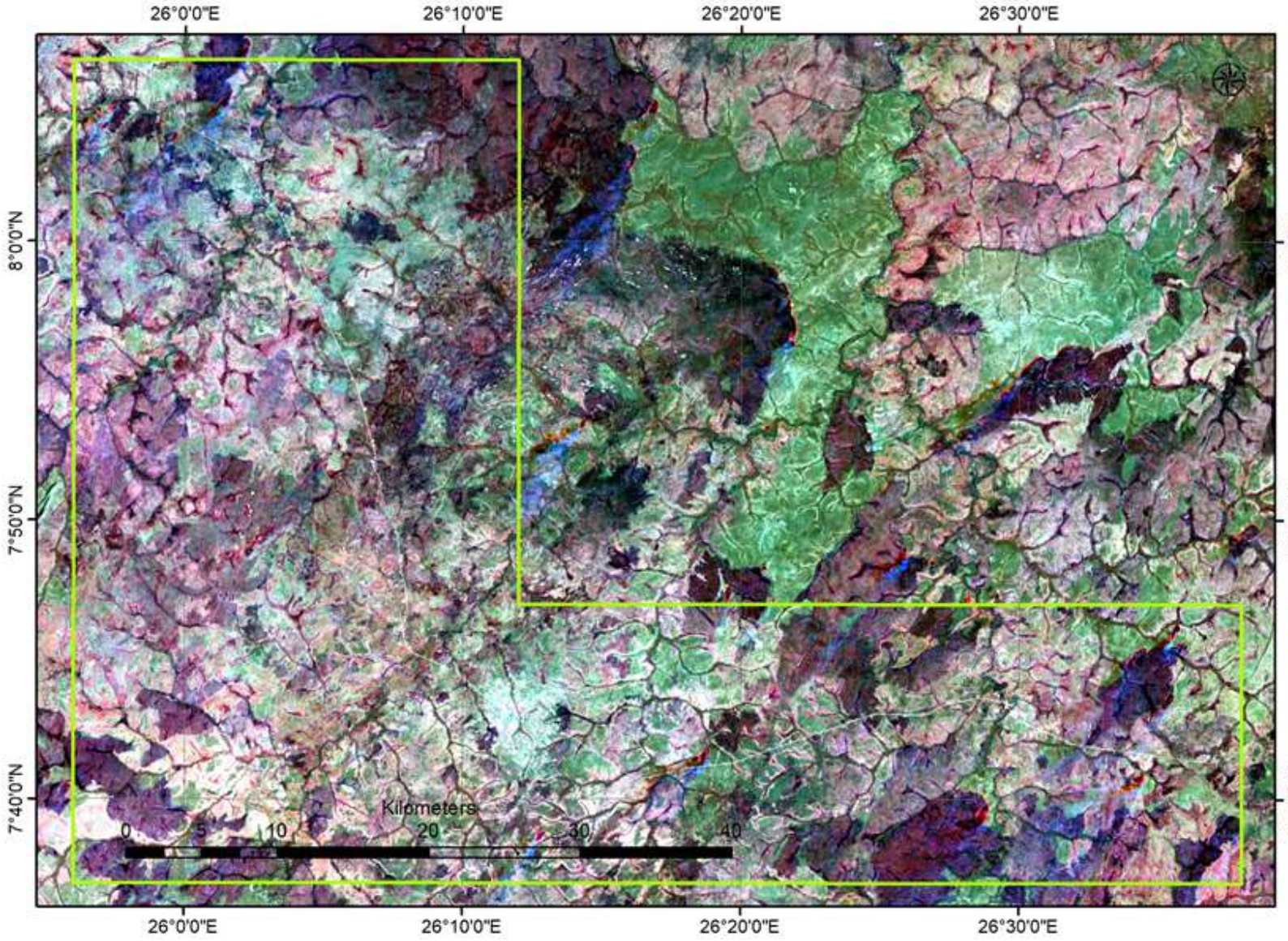

Fig. 3. Landsat7 ETM+ color composite images a) Linear stretched bands 7, 4 & 1 in R, G, B, respectively

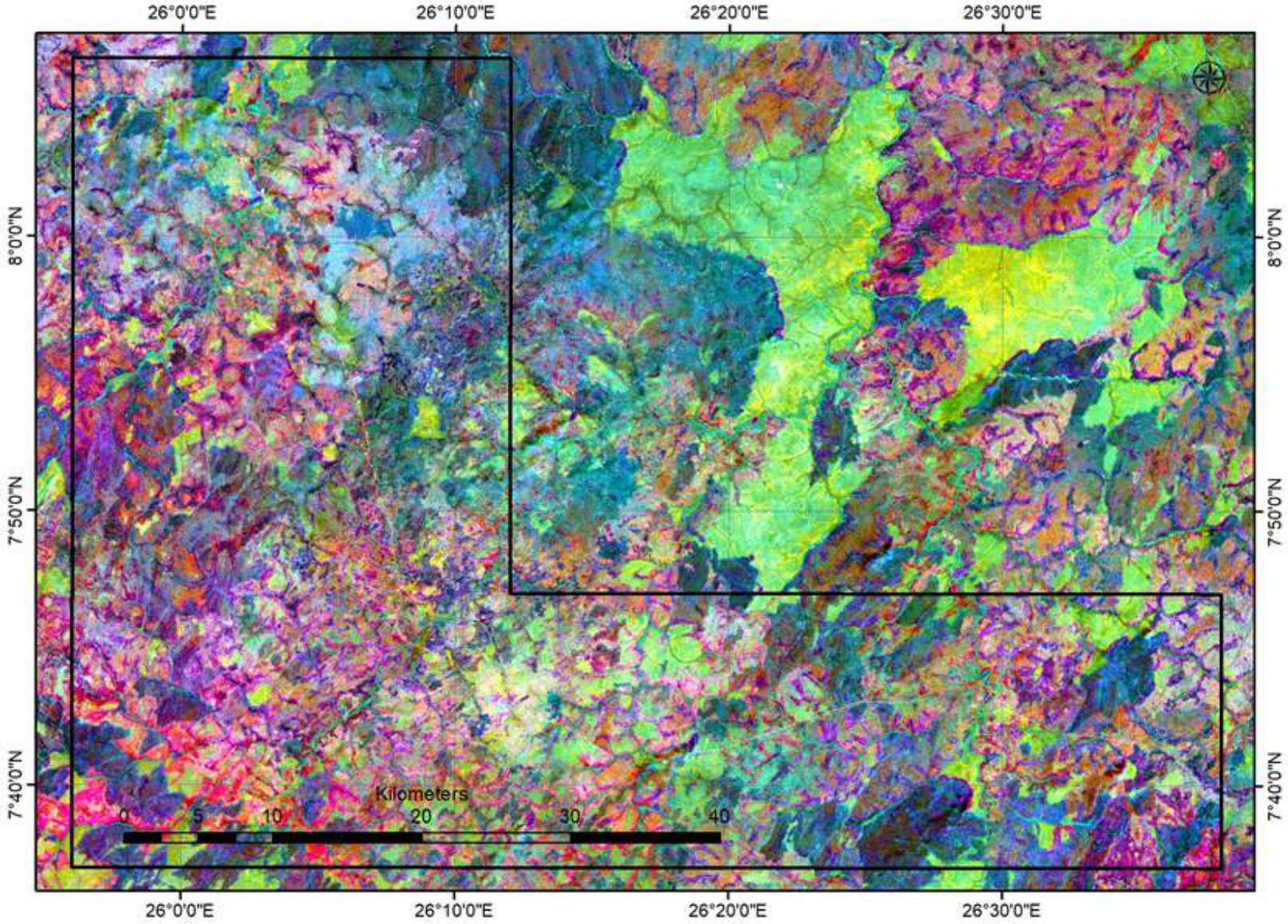

Fig. 4a. Landsat7 ETM+ color composite images, PCA 1, 2 & 3 in R, G, B, respectively

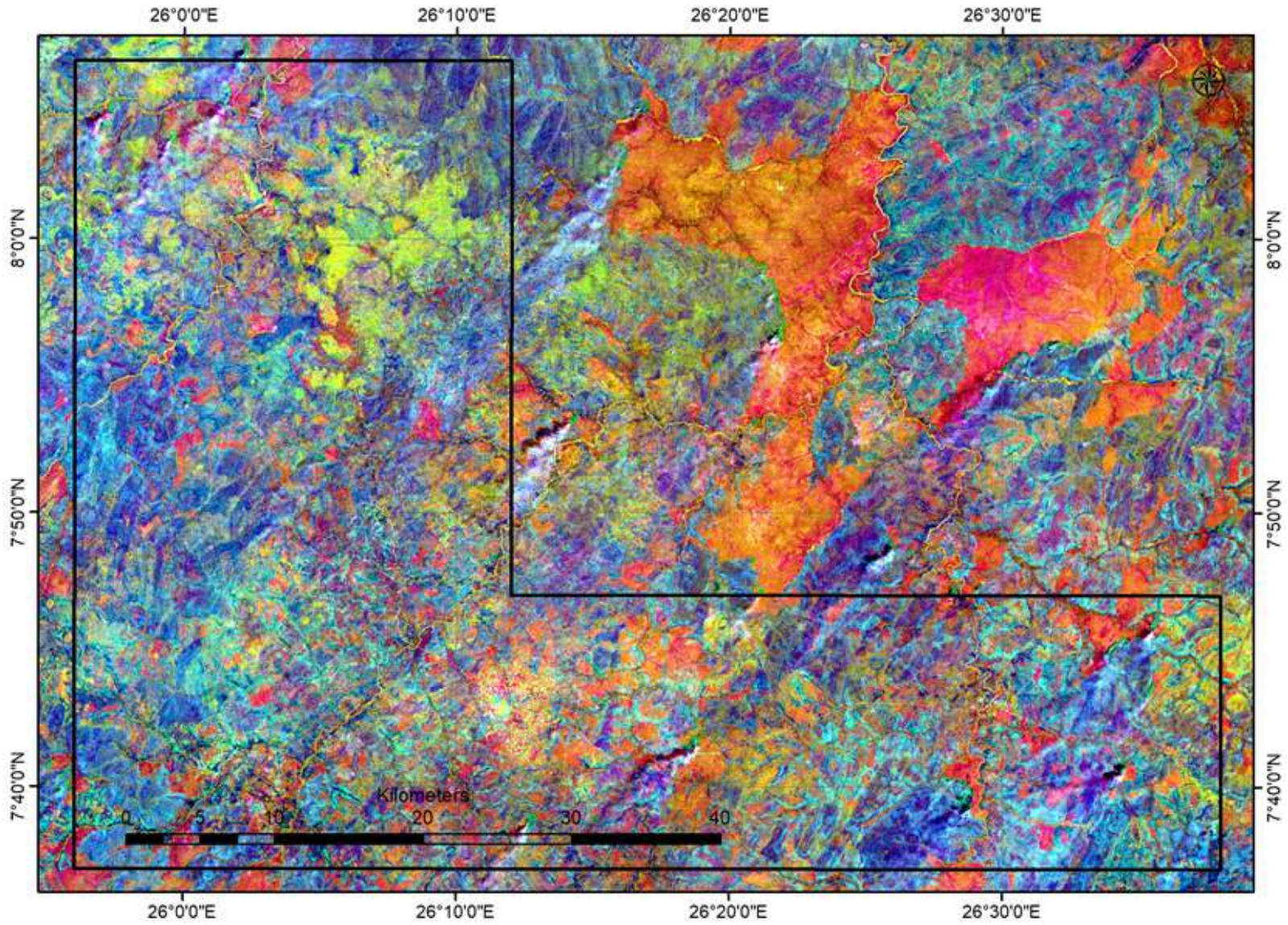

Fig. 4b. Landsat7 ETM+ color composite images, PCA 2, 3 & 4 in R, G, B, respectively

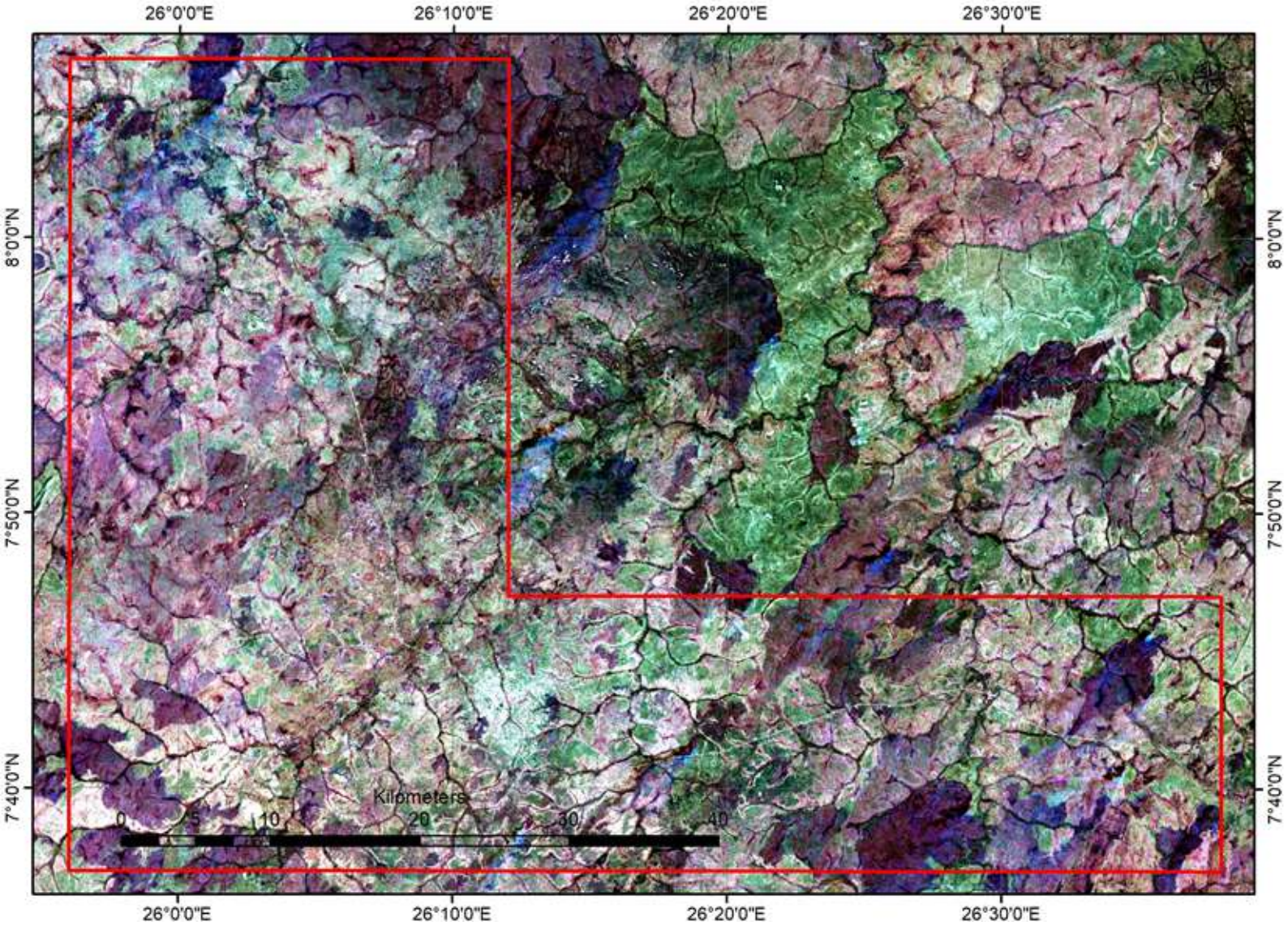

Fig. 5. Landsat7 ETM+ color composite images, Fused IHS of the DC bands 7, 4 & 1 with the panchromatic band 8

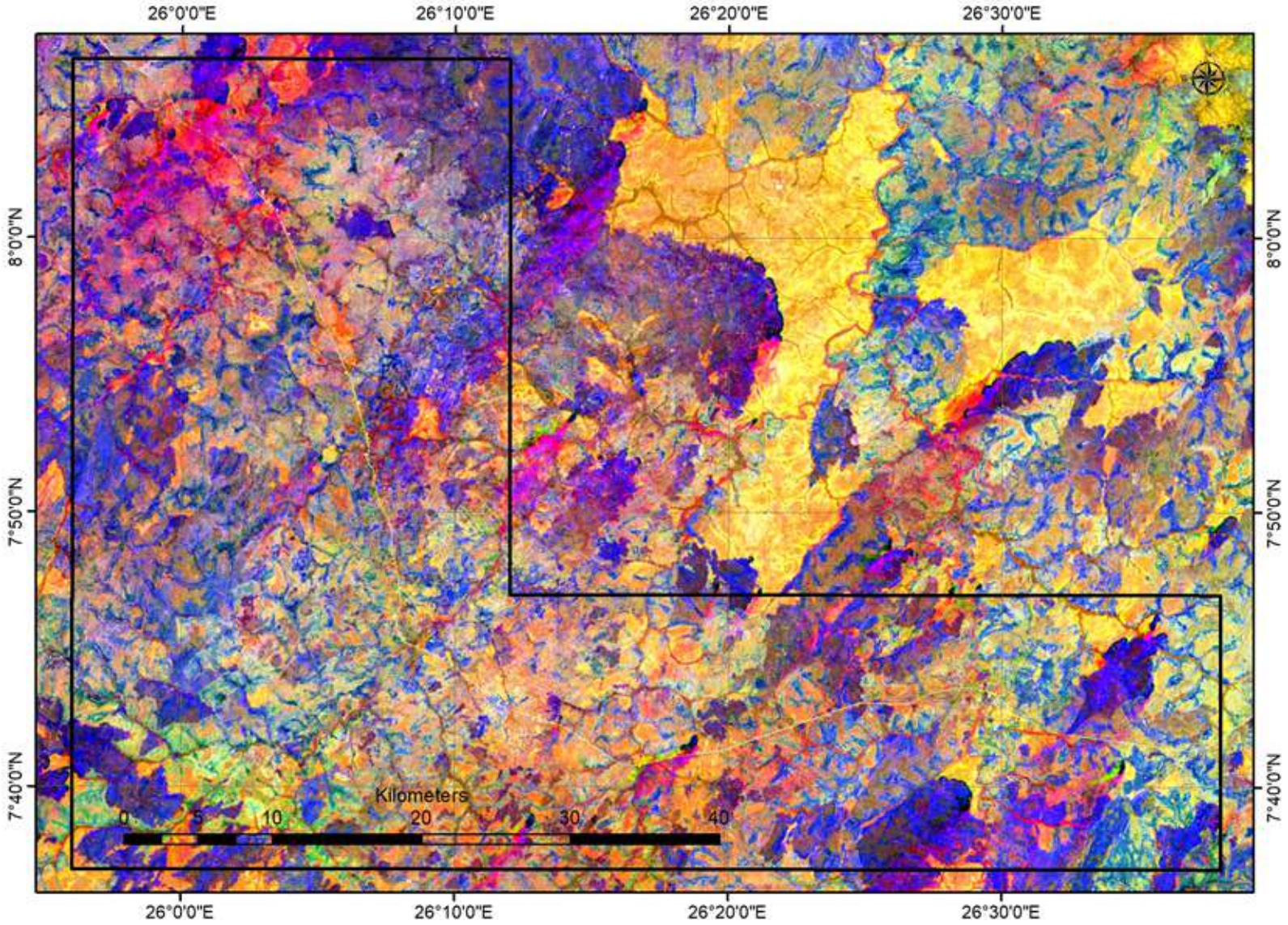

Fig. 6a. Landsat7 ETM+ color composite images, Band ratio bands 5/7, 3/1 and 3/5 in the R, G, B, respectively

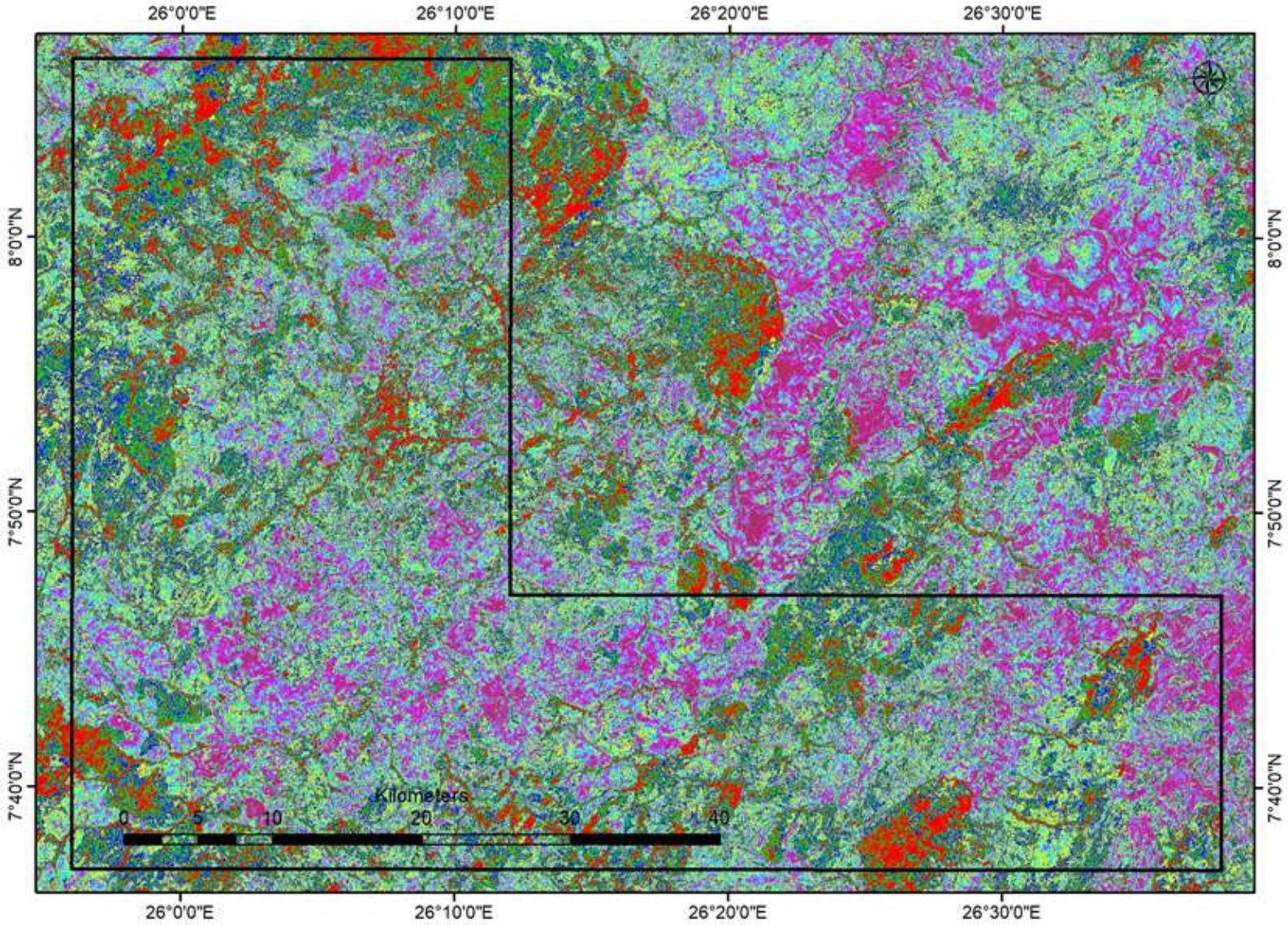

Fig. 6a. Sabins composite unsupervised classification of ETM+ data, a) Iso-data algorithm, b) K-means algorithm

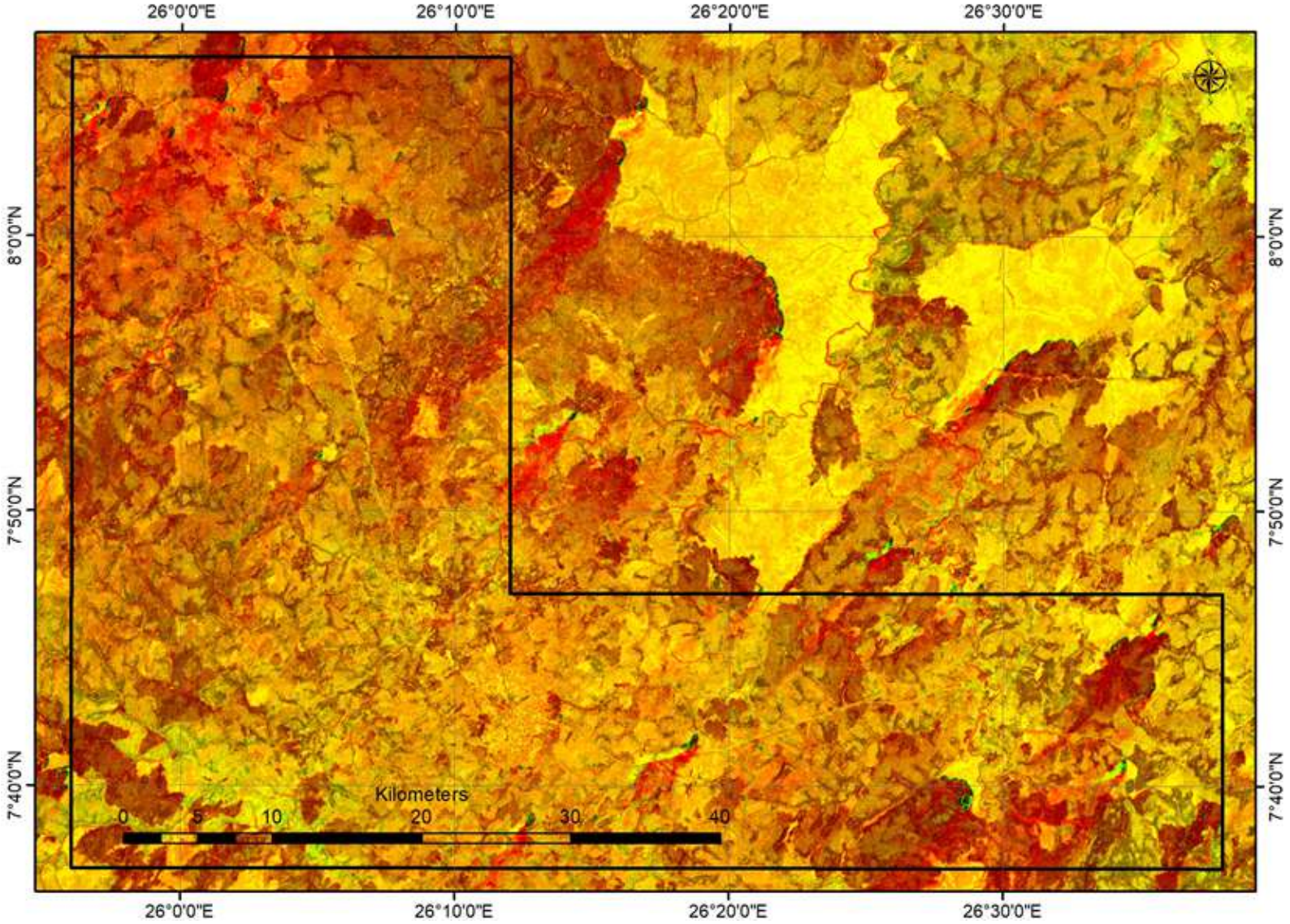

*Fig. 7a. Landsat7 ETM+ color composite images, Sultan's band ratio of bands 5/7, 5/1 and ¾*5/4 in the R, G, B, respectively*

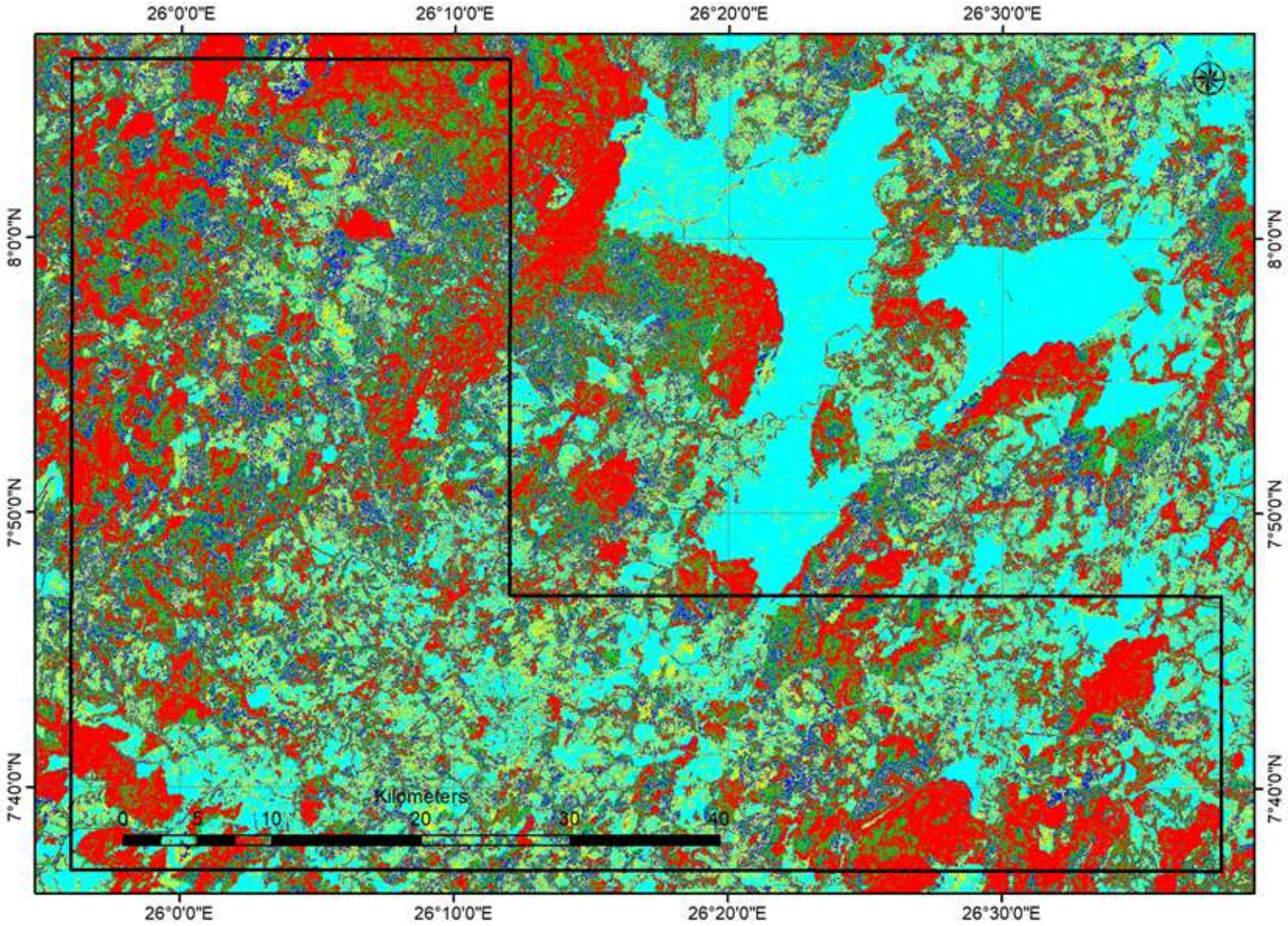

Fig. 7b. Sultan composite unsupervised classification of ETM+ data, a) Iso-data algorithm, b) K-means algorithm

Satellite images have been utilized to digitize the lineaments and drainage of the under consideration. Results are more or less conformable with the ones extracted from the DEM (Digital elevation Model) image of the SRTM data and GDEM from ASTER image. The digitized lineaments from satellite imagery have more than one trend; major and minor trends can be structurally analyzed after field measurements.

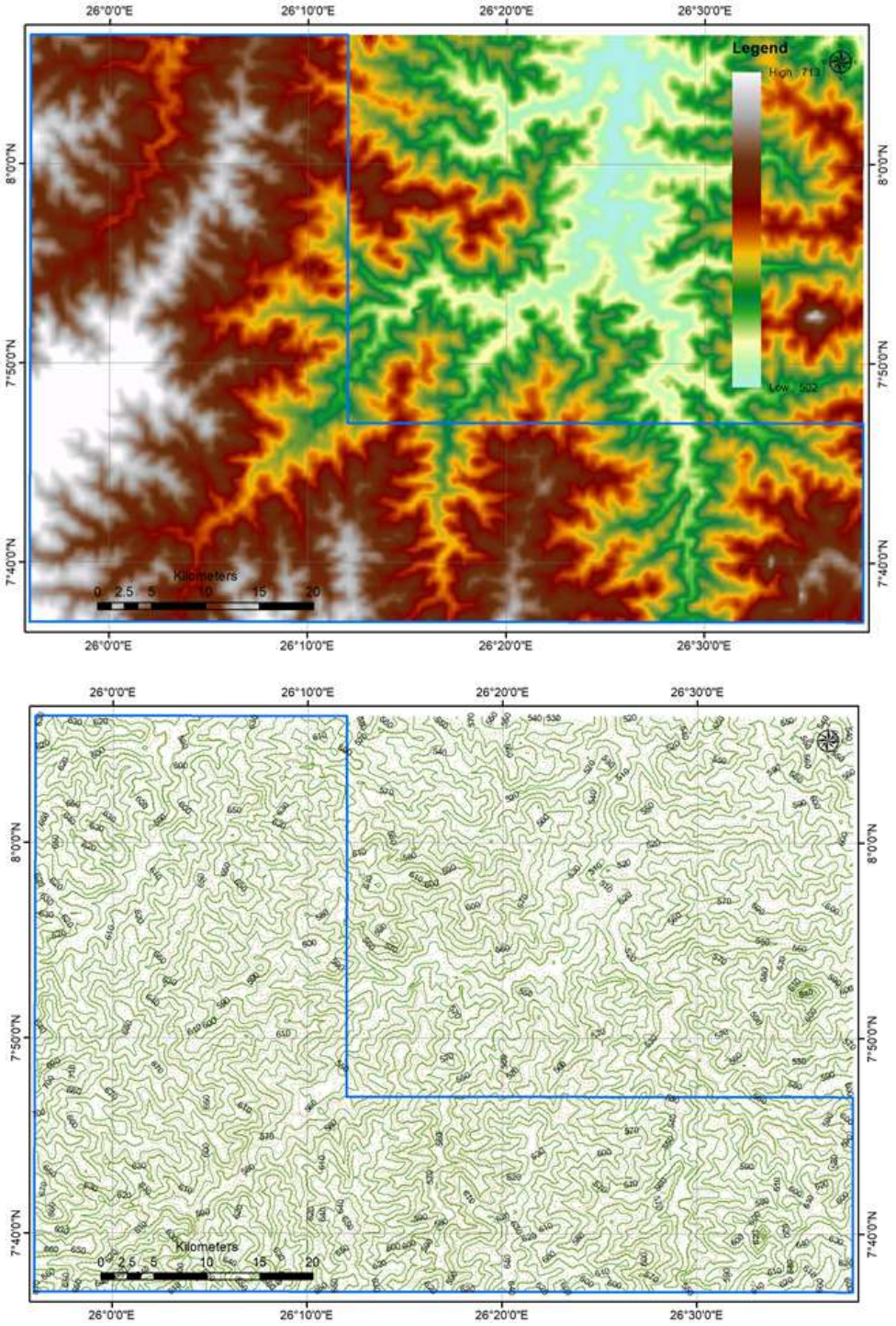

Fig. 8a. DEM image and contour line cover Block EL 21

Some topographic analysis was performed in this study. The present analysis focused predominantly on understanding the drainage patterns of the region and their connection to the topography as this will determine crucially the planning of future geochemical and geophysical surveys. The results of the topographic analysis are shown in Figure (8a).

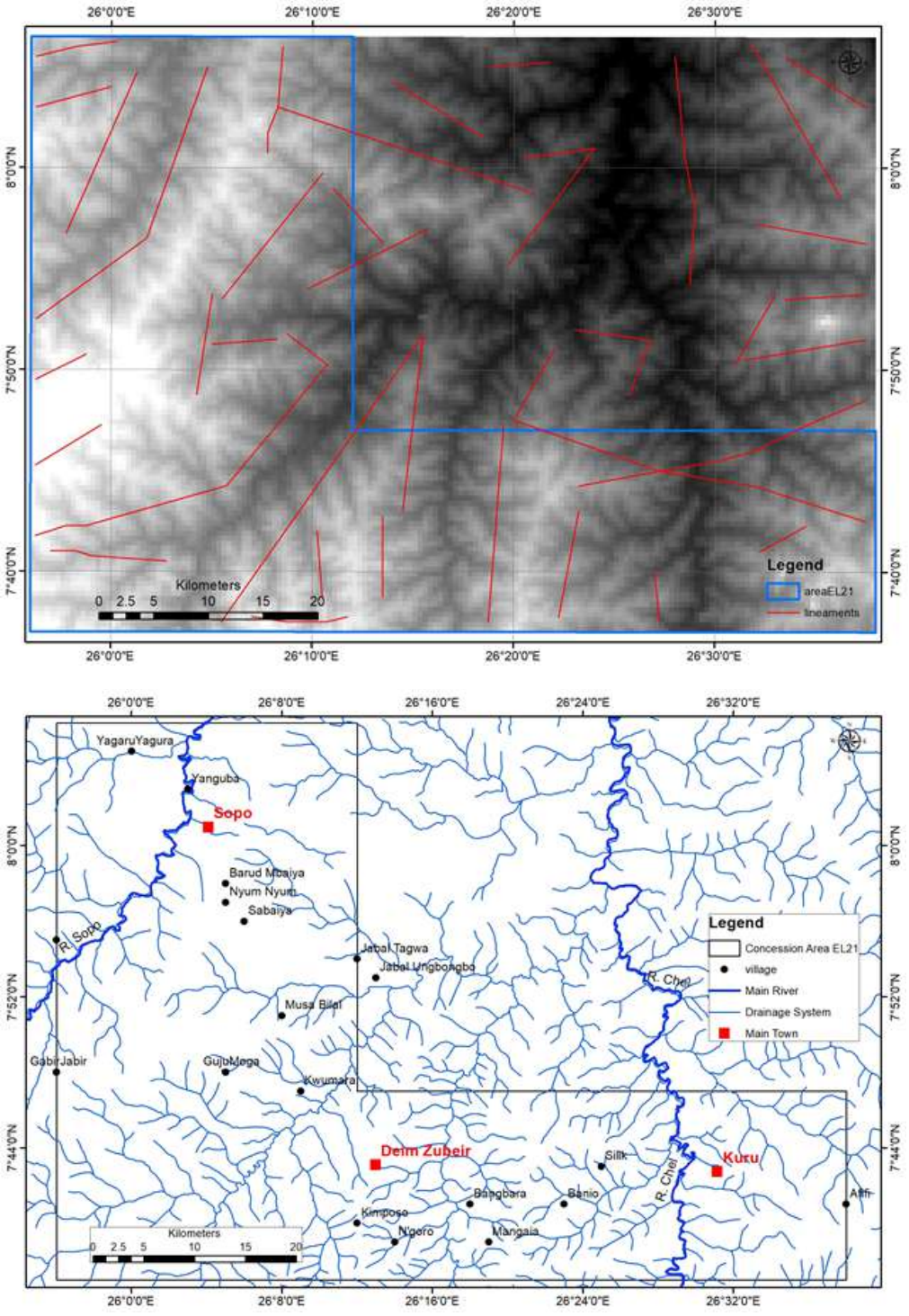

Fig. 8b. Drainage pattern and Lineaments maps of the study area

The surface elevation ranges between 700 and 500 m, whereas the general topography slopes towards the northeast. The region of highest surface elevation is located in the eastern part of the concession area. Topographic features like mountain ridges or incised valleys are characterized in the DEM image by a strong brightness contrast that is proportional to the topographic gradient and related to the direction of strike of the feature relative to the direction of illumination. In all presented maps the topography is illuminated by an azimuth angle of 300° and an altitude angle of 30°.

The drainage system revealed straight parallel drainage lines, which are controlled by the general structure manifested in the fault system in upstream these wadis exhibit feather-like drainage system (Fig. 8b). The drainage system and the watersheds of the region are extracted from the SRTM data. Individual channels are determined by applying Arc Hydro flow routing algorithm (and by the calculation of the upstream drainage area.

3. GEOLOGY & TECTONIC SETTING

3.1. Geological Setting

An overview of the regional and detailed geology as well as the geomorphological aspects in the project area is provided in the following sections. A systematic approach integrating, remote sensing data, field survey and literature review was employed. Landsat 8 and ETM+7 imagery for the project area, and area sheets from Atlas of the Sudan geological map at scale 1: 1000,000, produced by Robertson Research International and Geological Research Authority of Sudan were used for describing and interpreting the geological features and ultimately, to update the available geological map.

The lithological formation participating in the Wau region was differentiated lithostratigraphically into high grade biotite gneisses, metasedementary rocks, Volcano-sedimentary assemblages, Syn-Late orogenic intrusion, Post-Orogenic intrusions, Anorogenic intrusive rocks and related dykes, Quaternary recent alluvium (Figs. 9 & 10).

The country rock in the concession area, is comprised of metamorphosed old sediment and associated intrusive rocks, which are all presumably of Pre-Cambrian age. The rocks represented in the area include chlorite, schist, sericite schist, acid gneisses. Amphibolites and talc schists.

These rocks were subjected to intense shearing and shattering and the later mineralizing emanations, were injected along the shear planes. The ore in the mine is mainly chalcopyrite and pyrite occurring in a gangue of vein quartz and calcite. The mineralization is apparently associated with intense tourmalation, the ore on the oxidation zone, above the water table, (at 100, depth) is mainly malachite with minor chrysocolla and azurite. Gold was selected in the mineralized area together with some uranium minerals.

The gneisses are metamorphosed to the amphibolite facies of regional metamorphism. The magmatic high grade grey gneisses are highly folded, and intruded by syn-orogenic granitoids. Metasedementary rocks probably unconformably overlie these continental rocks. The gneisses are grey, migmatized, medium to course grained with distinct mineral location fabric. The gneisses composed of quartz feldspar, biotite, hornblende, muscovite, and sometimes almandine garnet. Chemically, the gneisses are granodiortic in composition and the gneiss in area is probably metasedimentary in origin. The age of these basements

is unknown. By analogy with similar gneisses elsewhere it seems likely to be of Mid-Lower Proterozoic or older.

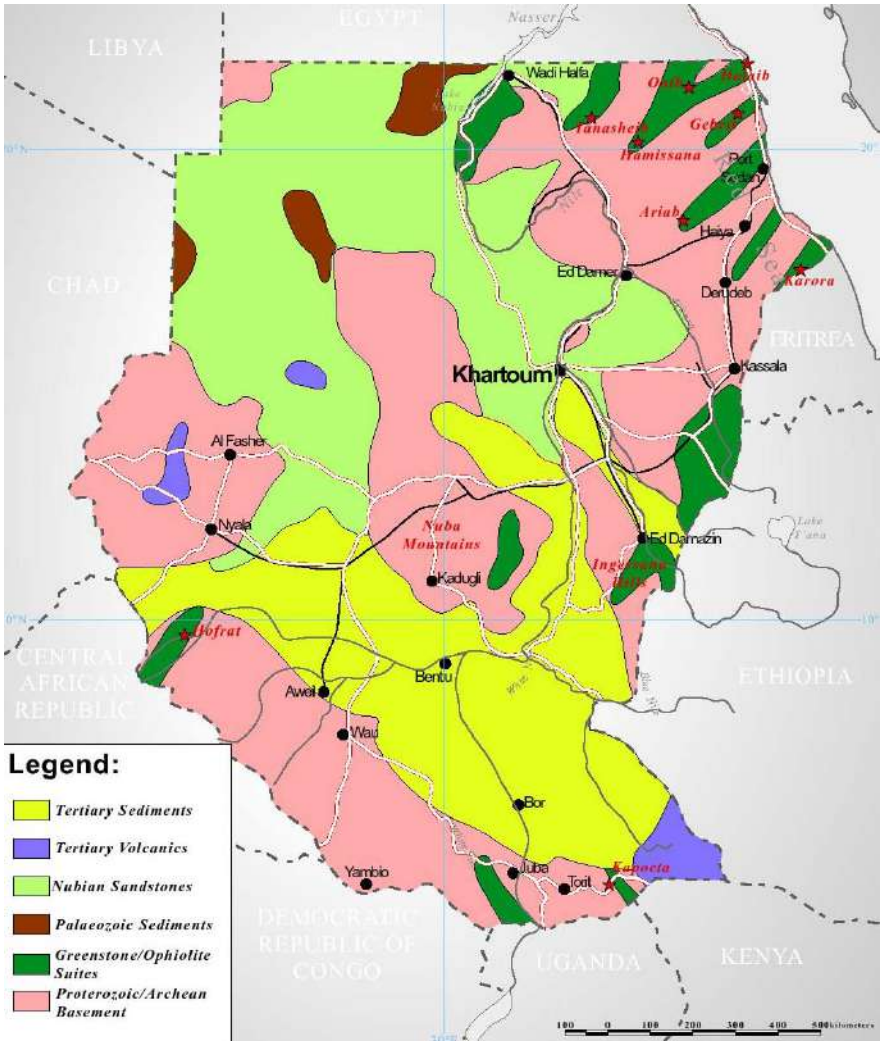

Fig. 9a. Geology and main mineralised belts of the Sudan and South Sudan

The metasedimentary unit is predominating into localities in the study area. The metasedimentary containing Para-gneisses, pelitic and semipelitic schist, marbles, and calc – silicates, all indicative of a shelf environment, now in amphibolites to granulite of regional metamorphism. The metamorphic grade of metasediments is high amphibolite to granulite facies and assigned to the Lower Proterozoic age.

Associated with the volcano- sedimentary assemblage lenses of mafic-ultramafic rocks. The Mafic-Ultra rocks were located in the regions; poorly exposed ultra-mafic bodies represented them.

Pan- African volcano- sedimentary rocks cover the study area. It's observed from the core logging data that volcanic rocks are in direct contact with the high grade gneiss rocks characterized by zone of thrusting and mylonitization.

The post orogenic intrusions occur as non-deformed intrusions and related dykes. Often they have already been made of the white, granitic dykes in Chel River near Deim Zubeir village.

The quaternary-recent alluvium deposit cover consists of residual soils, laterite and sheet talus occupy nearly all the plains and effectively conceal the bedrock formations. The alluvium is extensive and relatively thick along Umbelacha River, Khor Yirongo and their tributary streams. Where seen it consists of vaguely and coarsely bedded reddish clays, containing variable amounts of fine sands and concretionary bodies principally of lime, no sharp line between alluvium and residual soils was observed and it seems probable that some of the superficial materials, away from the sometimes ill-defined stream courses, is also of alluvial nature, having been transported to some extent by sheet floods. Laterite is widespread and apparently extensive in some localities. It generally forms sheets of aggregated botryoidally concretions, a quarter to half an inch in diameter. Laterite sheets from more than 5 m thick, are present at several places in Chel and Sopo Rivers.

3.2. Tectonic Setting

The study area occupies an important region in the East African Orogeny since it is exposed close to the interface between the Arabian–Nubian Shield in the north and the Eastern Granulite belt to the south which represent part of the Mozambique belt (Fig. 9). The exposed part of the shear zone in Uganda seems to separate Precambrian regions that differ in their characters. The region to the southwest of the shear zone is dominated by the Northern Uganda terrane (Fig. 9) which is composed of Mesoarchean granulites and Neoarchean gneisses, migmatites, and granitoids (Nyakecho and Hagemann, 2014; Westerhof et al., 2014). The northern part of this terrane is intruded by a largely un-deformed Neoproterozoic granitic body. Differently, the region to the northwest of the ASZ is characterized by the presence of Neoproterozoic exposures of banded granulites–charnockites complexes together with highly sheared Neoproterozoic gneisses and granitoids, and Archean Paleoproterozoic gneisses (Nyakecho and Hagemann, 2014; Westerhof et al., 2014). Westerhof et al. (2014) concluded that the Neoproterozoic granulites–charnockites complexes are tectonically emplaced and they represent three allochthonous sheets referred to as the Morungole, Akur and Ukatat massif (Fig. 9). These allochthonous sheets were thrust above the Archean–Paleoproterozoic gneisses. Further, Westerhof et al. (2014) proposed that the source of the Neoproterozoic banded granulites–charnockites allochthonous sheets is the deeper roots of the suture between East and West Gondwana. Fritz et al. (2013), Westerhof et al. (2014) and Nyakecho and Hagemann (2014) agreed that the Neoproterozoic rocks in the northeastern-most part of Uganda belong to the East African Orogen. Westerhof et al. (2014) referred to these exposures as the Pan-African Karamoja belt (Fig. 9).

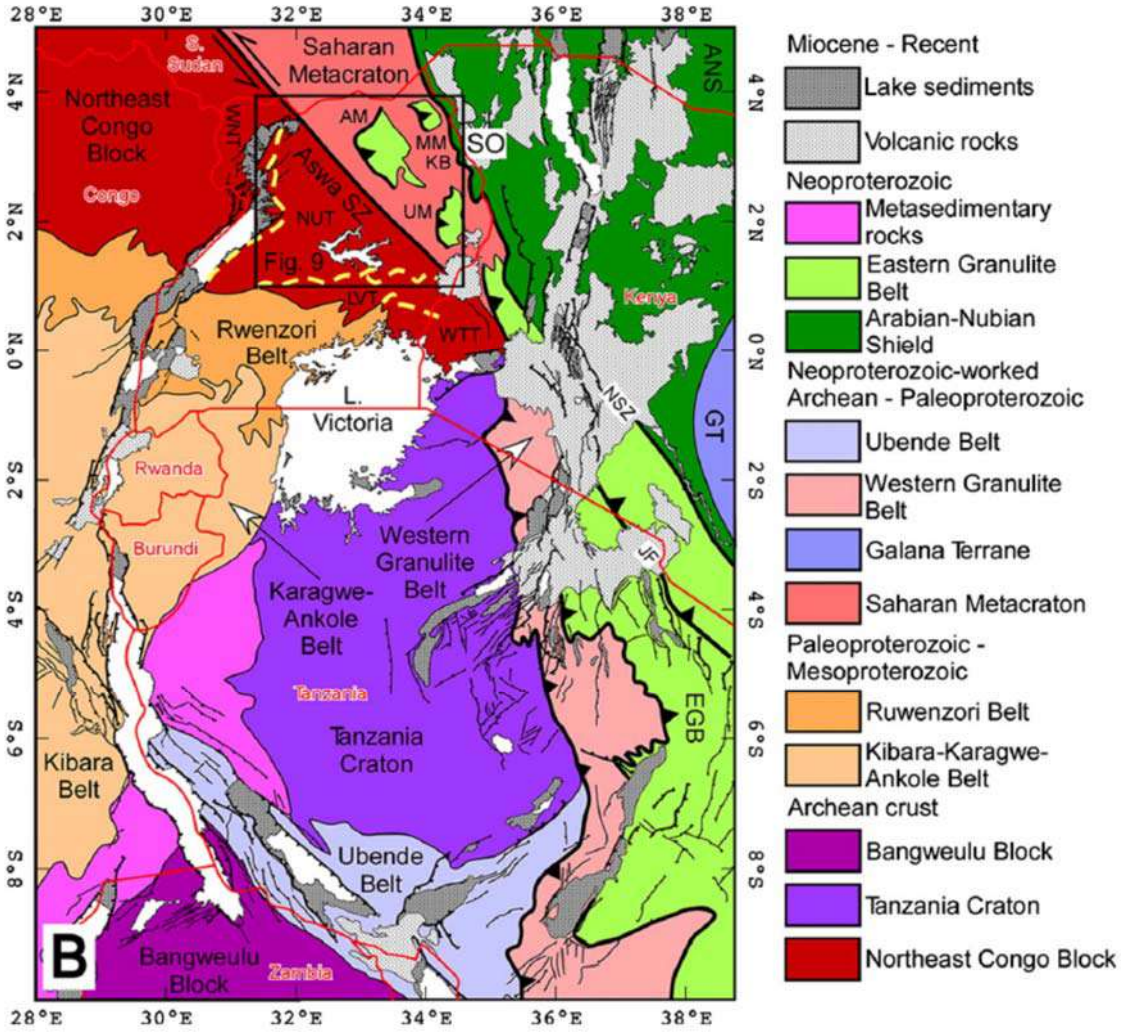

Fig. 9b. Precambrian tectonicmap of eastern Africa. Modified from a compilation by Katumwehe et al. (2015). Dotted yellow lines approximate the boundaries suggested by Westerhof et al. (2014) to divide the Northeastern Congo block in Uganda into the Western Nile terrane (WNT), Northern Uganda terrane (NUT), Lake Victoria terrane (LVT) and West Tanzania terrane (WTT). ANS = Arabian–Nubian Shield. GT = Galana terrane. EGB=Eastern Granulite belt. SO=Sekerr ophiolite.MM=Morungole massif. AM=Akurmassif. UM=Ukutatmassif. KB=Karamoja belt. NSZ=Nyangere shear zone. JF=Jailhouse rock fault.

The basement complex series were the only rocks affected by major tectonics. The quartzitic series of Bahar Kwadjia were subjected to folding but the movements were weak. There were no observed signs of friction or violent shearing, normal in the case of basemen rocks. The general trend of the axis of folding is N.N.E.- S.S.W.

There is also a vast zone of mylonitization, which affected principally the quartzites of Sopo in these mylonitized areas, indications of the existence of gold deposits were found. However, the accompanying regional structural map represent the major lineaments (Fig. 10). Quartzites are dominant along the whole watershed and constitute the majority of the elongated ranges of hills to the cast of Chel river. Some of the quartzites are very pure,

some contain varying proportions of tiny flacks of muscovite or sericte and some are ferruginous. Chlorite schists biotite schists and quartz sericite schists occur in scattered outcrops, usually occupying rather Flattish land or low hillocks. The schists are most probably of much wider extension the thought, but they are mostly concealed by the superficial formation. Marble is recorded in Khor Kuru.

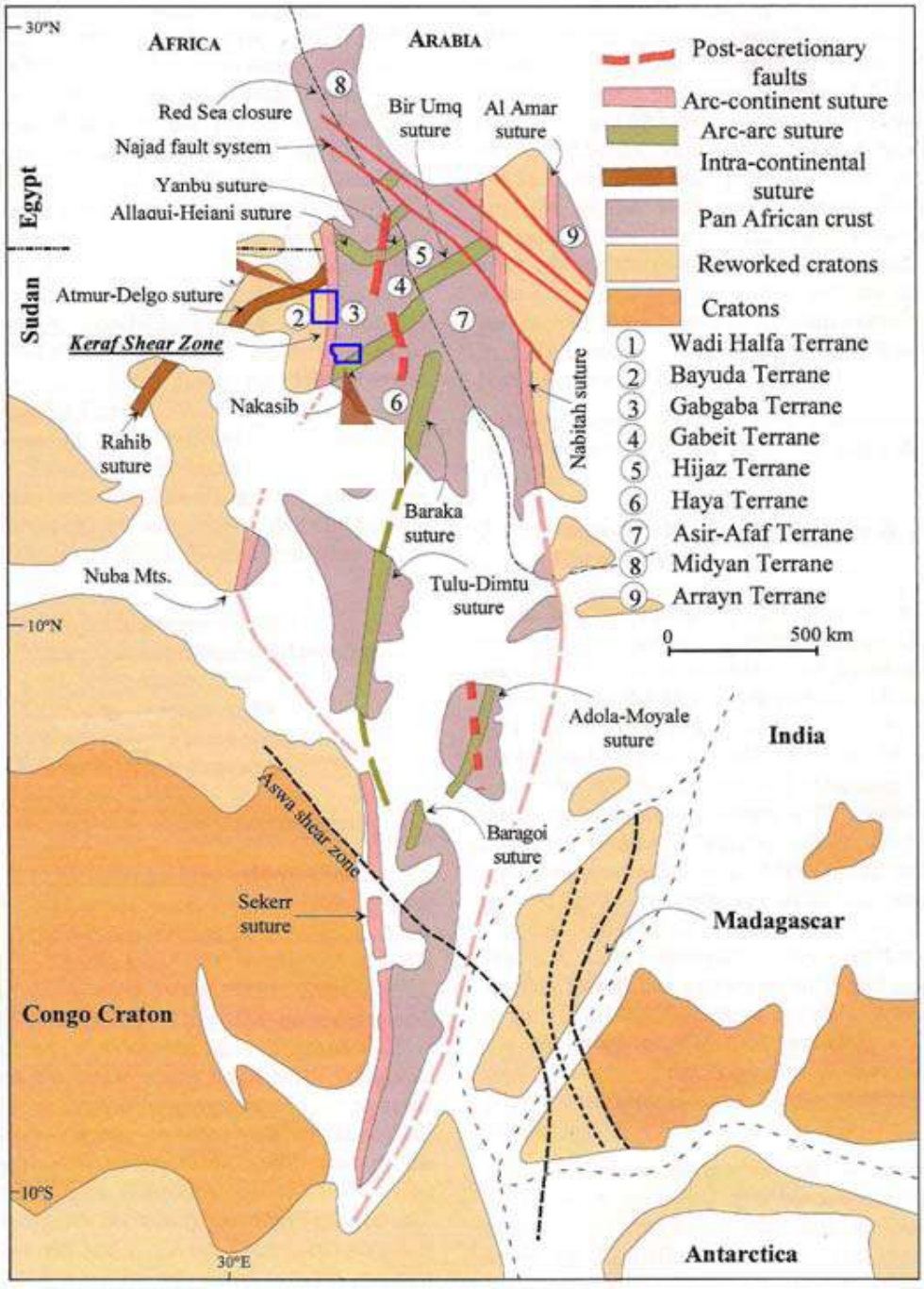

Fig. 9c. Tectonic and geological context of the project area (modified after Stern, 1994)

The regional trend of foliation as common to both schist and quartzites, ranging from N.N.E- S.S.W. to N.S. with local anticlines and syncline. The age relation between the different metamorphosed formations is not quite clear yet. There is a series of parallel shearing zones, trending generally N.E.- S.W. and extends from beyond the northern limit of study area, in a south westward direction to J. Tagwa, J. Ungabongbo and J. Kuru, to beyond Khor Kuru in the southeast of block EL 21. The zones are characterized by intense silicfication which occupies the prominent ridges on the crests of the hills the zones of shearing were also used as channels for the introductions of boron emanations into the surrounding rocks. The quartz veins and the quartz-cemented conglomerate are of a semi regional distribution in the whole area. The dominant Varity of tourmaline is the black schorl. Tourmalinization, due to pneumatolitic action, is observed on the wall rocks around the shear zones with varying degrees and some slides of quartiz-sericte schist show the two minerals in very fine grains; these are intruded by multitudes of stringers of well-developed tourmaline prisms with quarts. More advanced degrees of Tourmalinization were also observed, where all the minerals in the rock, except the quartz, were attacked by boron emanations, with the formation of tourmaline. This widespread Tourmalinization could possibly be related to the granite intrusions exposed in several localities. In J. Nimbi the rock is medium grained, grey granite. (orthoclase and oligoclse). Biotite exists in elongated, non-oriented tribute. Apatite is also present as an accessory minerals ironstone.

Another point of interest concerning the regional geological of the area is the very extensive occurrence of ironstone. This is found practically in every plain land, in Bahar el Ghazal State, either directly exposed or covered by a thin mantle of dark soil.

3.3. Lithostratigraphic units

The lithologies that comprise the study area are characterized by an abundance of high grade gneisses, metasedementary rocks, Volcano-sedimentary assemblages, Syn-Late orogenic intrusion, Post-Orogenic intrusions, Anorogenic intrusive rocks and related dykes, Quaternary recent alluvium. Generally, the study area has revealed the following lithostratigraphic units:

a. Meta-sediments of pasanumo-pelitie constitution and calcareous psammo-pelites.
b. Metamorphosed schists of intermediate to basic composition, probably after diorites and gabbros.
c. Metamorphosed rocks of ultra-basic composition
d. Acid gneisses partly porphyroblastie
e. Granite pegmatities, aplites and rather fresh granites

Lithostratigraphic units	**Age**
Acid gneisses	Archean to middle Proterozoic
Metasedementary rocks	Lower Proterozoic
Volcano-sedimentary assemblages	Upper Proterozoic
Syn-Late orogenic intrusion	Late orogenic
Post-Orogenic intrusions	Mesozoic
Anorogenic intrusive rocks and related dykes	Phanerozoic
Quaternary recent alluvium	Quaternary

A. The acid gneisses are represented by the following assemblages:

- Porphyroblastic quartz-feldspar gneiss.
- Tourmaline-epidote-quartz-plagioclase gneiss
- Muscovite-biotite-quartz-feldspar gneiss
- porphyroblastic chlorite-epidote-quartz-plagioclase gneiss.

The acid gneisses are mainly formed of quartz and feldspar. The grain size is dominantly coarse, and a common feature is the presence of feldspar in a porphyroblastic texture/ quartz generally shows signs of destruction and partial re-crystallization with sutured outliners. Feldspars are mainly orthoclase accompanied by a certain proportion of oligoclse. The feldspars show partial crushing and sericitization specially around the bigger grains which stood the action of stress. Kaolinization strongly affected the a few cases tiny flakes of muscovite and biotite could have traced, arranged in parallel alignment. Tourmaline in tiny stringers was seen in many sections of this acid gneiss.

B. The group of meta-sediments include the following assemblages:

- Plagioclase-quartz-chlorite schist.
- Chlorite-epidote-sericite-plagioclase-quartz schist quartz-sericite schist
- Epidote-chlorite-quartz-sericite schist.
- Sericite schist quartz-chlorite-sericite schist
- Epidote-quartz-plagioclase chlorite schist.
- Quartz-chlorite schist
- Epidote-quartz schist

The meta-sediments studied, include metamorphosed psammites and psammo-pelites, which are partly calcareous. Quartzite, sericite quartzite and epidote-quartz gneiss represent the more psammites types. The schists of psammo-pelites composition are represented by sericite and chlorite schists. The meta-sediments are generally very fine grained, highly foliated and varying in colour form light creamy shade to light grayish green. Chlorite-sericite schist is a common type, displaying a phyllitic texture.

C. Volcano-sedimentary assemblages were recognized:

- Calcite-quartz-chlorite schist
- Biotite-chlorite schist
- Quartz-plagioclase-chlorite schist.
- Quartz-plagioclase-biotite-chlorite schist
- Quartz-epidote-chlorite schist
- Epidote-biotite-chlorite schist
- Actinolite-chlorite schist
- Chlorite-biotite-amphibole schist
- Quartz-chlorite-feldspar-actinolite schist
- Biotite amphibolite
- Quartz-feldspar-hornblende gneiss

- Quartz-feldspar-biotite-hornblende gneiss
- Chlorite-plagioclase-hornblende schist
- Quartz-feldspar-biotite schist
- Quartz-plagioclase-chlorite-biotite schist
- Biotite-quartz-epidote-feldspar rock.
- Epidote-hornblende-sericite-quartz schist

In the hand specimen the rocks are fine grained to medium grained, foliated and generally hard and compact. Their color varies between dark grayish to greenish. They are normally jointed and show slicken siding. Chlorite schist, amphibolites, amphibole schists and biotite schist represent them.

The chlorite schist is formed and lathes and prisms of chlorite, generally in alerting bands with grains of plagioclase in varying proportion. The plagioclase in dominantly of the labradrite composition, and is usually, always sansseritized with the formation of epidote and zoisite. The grains of plagioclase may be occasionally porphyroblastic.

Calcite is present in ramifying stringers, sometimes in noticeable concentrations. Sphene is present in most of the rocks examined, and occasionally sometimes as an accumulation of fairly big crystals. Quartz takes a minor part in the composition of these rocks and when present it is always interstitial and shows strong undulose extinction.

Biotite is present in tiny shreds in some varieties of the chlorite schist, when present, it is aligned in parallel rows, giving a distinct schistosity to the rock chlorite is always related to biotite as its alteration product. When biotite becomes the dominant mineral, then the schist could be called biotite schist. Quartz is also present in some of these rocks but in ordinate amount.

The presence of hornblende is sometimes this assemblage generally occurs in medium to coarse grains, with a gneissic structure. The plagioclase average around labradorite in composition and in not much altered. Hornblende, sometimes of the actionlitic variety, is the normal and dominant mineral in this rock, and in some cases it is a product of the hydrothermal uralitization of the original pyroxene. Amphibolites are compact dark greenish rocks which show no foliation under the microscope. They are formed of rather big imbricating lathes and prisms of hornblende, with plagioclase feldspar as a minor constituent. the rock may be cavernous, with prochlorite filling the cavities in radiating flakes. Chlorite may be related to the amphibole as an alteration product, and it is then dusted with specks of iron oxide.

D. The group of granites includes the following:

Normal coarse granite, pegmatite and micro-pegmatite Biotite-tourmaline-microcline granite. In this group, granite is rather rare in occurrence compare with the other members. In the hand specimen it is pinkish in color, medium grained and compact. It is composed of quartz, orthoclase, microcline grains show that they have undergone stress to a certain extent. Alteration of the feldspar was noted. The accessory minerals present are mostly apatite, zoisite, few tiny grains of zircon and occasional sphene crystals. Tourmaline occurs as an original mineral in the rock in varying abundance

Pegmatites are nearly of the same composition as the granites but have a much bigger grain size, and show the effect of stress more distinctly. They are in the form of veinlets and stringers, cutting across the other groups of rocks. Tourmaline is very abundant in these veinlets, occasionally being associated with dense concentrations of sulphides.

3.4. Mineralization

The majority of the mineralised occurrences within the study area have been located within these 'greenstone-type' units, and in particular, felsic volcanics. More advanced lithological mapping, aided by satellite imagery interpretations, has also suggested a further division of the 'greenstones' into block EL 21 has been recognised to be most important for the potential discovery of commercial gold and alteration mineralisation zone (Fig. 13). Three principal forms of metallic mineralisation have been identified:

a) Massive sulphide (Cu, Pb, Zn, Au, Ag) and silica-barite (with Au) mineralisation occurring in both volcanogenic island-arc and axhalative sedimentary environments.
b) Mineralisation in collapse breccias and recrystallised host rocks related to tectonic, intrusive and metamorphic episodes.
c) Mineralisation related to shear zones and vein systems.
d) The ore lodes: The upper levels of the ore lodes are occupied by the zone of oxidation. The outcrops do not represent the true widths of the lodes accurately, being somewhat exaggerated. This is due to the high solubility of malachite, and the wider dissemination of copper staining by surface waters. The mineralized zone tapers, then the little below the surface till the level where the sulphides begin to appear, then the width becomes uniform in depth. The level at which the sulphides begin to appear few meters below the surface. The ore in the zone of oxidation is in the form of a cementing material to the brecciated country rock and stringers and congnised in the zone of oxidation (Malachite-azurite-chrysocolla-cuprite-chalcocite-native copper-hematite-limonite-siderite).

3.5. Geomorphology

One of the main benefits of carrying out a remote sensing interpretation to construct a lithostructural interpretation map is the improved level of structural geological detail that is generated to place the targets which have been identified in their geological context. In addition, these data assist in the interpretation of future geochemical and geophysical surveys, and as it has been captured digitally on a GIS it can be added to the exploration database for the region.

The main structural features that have been mapped in this area are as follows:

- Foliation and bedding traces (The regional trend of foliation as common to both schist and quartzites, ranging from NNE-SSW to N-S)
- Faults and fractures (trending generally NE-SW)
- Highlighted faults and lineaments on the structural synthesis map (general trend of the axis of folding is NNE-SSW) (Figs. 8, 9, & 10)

The belt of gneisses along the international border, extending into gneissic terrain north of study area. These gneissic terrains can thus be regarded as ancient continental blocks, but they have been subsequently metamorphically over printed and tectonically reworked.

The meta-sediments unit is appearing to have been unconformably deposited over the continental gneisses. These meta-sediments and the underlying gneisses have been subjected to high grade of regional metamorphism reaching upper amphibolite facies. The volcano-sedimentary separated from the high grade rocks by a major thrust zone along which mylonitization, crushing and tectonization have occurred.

The contact between green schist volcano-sedimentary assemblages and high grade gneisses in the vicinity of Wauis zone of highly mylonitized, sheared and intensely deformed rocks up to 5km wide and probably over 300 km long.

Quartzo- feldspathic rock in ribbon like bands associated within thin bands of talc and graphite schist, foliated, crushed rocks predominates in the mylonite zone. These strongly developed bands of tectonics probably mark wide strike-slip shear zone, or ramped thrust, (Vail et al., 198). These assemblages are all now folded and faulted along similar structural trends up right NE trending isoclinal folds affect all of the stratigraphic units.

There are two main foliation trends in the COIPA concession area:

- NNE-SSW and NW-SE. The dip is moderate to the N.W. the shear zones and fault planes are directed N. 60 E., N. 45 E., and N. 25 E.
- In the study area faults are of three main trends: NW-SE, NE-SW and N-S. By examining the sections drawn for the mineralized lodes occupying the north and south shear zones, one feels justified to assume that the southern plane of shearing is dipping steeply north westwards, while the northern one is dipping steeply south eastward and auriferous quartz veins considerable structural control of the gold mineralization in study area.

Another feature of the centeral part of the area is the occurrence of veins large enough to be seen on the satellite imagery, suggesting that they might be more than 10 m in width in some places these form linear positive features and in some instances they may represent silicified fault zones or breccias.

The structural synthesis map has the Landsat image as a background and this has been toned down by 30%, the foliation traces and all faults are shown over the Landsat image. On top of this background major fault trends have been highlighted and major lineaments have been added. Some of these have to be inferred either by linking short segments of faults or where likely structures are concealed by wadi sediments the lineaments have been inferred. These highlighted faults and linear show that there are a number of structural zones with varying trends to foliation and bedding, these blocks appear to be controlled by the large late syntectonic granitoids that underlie large parts of the area.

The lithological units have been mapped on the basis of their geomorphic appearance and their expression on the ASTER and Landsat imagery and are summarized below in Table (2).

Table 3: Satellite Image Expression of Geological Units

LITHO-UNIT	Lithology	image EXPRESSION
Quaternary Holocene	Alluvium & wadi sediments	Narrow light toned smooth textured beds to the major wadis with indications of active alluvial flow including coalescing braided streams
Quaternary Holocene	Colluvium, fans, terraces, sands & gravels	This unit is made up of a range of surficial deposits: dark toned alluvial fans; dissected cemented terraces & very dark colored black cotton soil with low relief
Age Unknown	Dolerite dykes	Dark toned, linear often with positive relief forming ridges up to 10 km in length, but generally shorter.
Late Proterozoic PZgr	Undifferentiated syn-late orogenic intrusive	Generally, light toned recessive units, covering wide areas with moderate to low relief & weak dendritic drainage. Gradational contacts with poorly developed foliation, & often intruded by dyke swarms.
Late Precambrian IUg	Younger granites	Ovoid shapes, sharp contacts; areas of moderate to high relief & distinct tonal anomalies on the 'Sultan' ratio images. Except the very light toned, low relief lenticular granite with roof pendants in the southeast Block
Proterozoic PLq	Metasedementary rocks	Narrow light toned smooth, strongly foliated areas of well developed 'strike ridges' & moderate relief with grey to mottled tones forming east-northeast to northeast oriented belts in the basement.
Proterozoic PLP	Volcano-sedimentary greenschist assemblage	Strongly foliated areas of well developed 'strike ridges' & moderate relief with grey to mottled tones forming east-northeast to northeast oriented belts in the basement.
Proterozoic PLu	Undifferentiated metamorphic rocks	Zones of massive, weakly foliated rocks with moderate relief mainly occurring in the northwest block. These undifferentiated metamorphic rocks to basic volcanics can be picked as very distinctive units on the Sultan' ratio images.

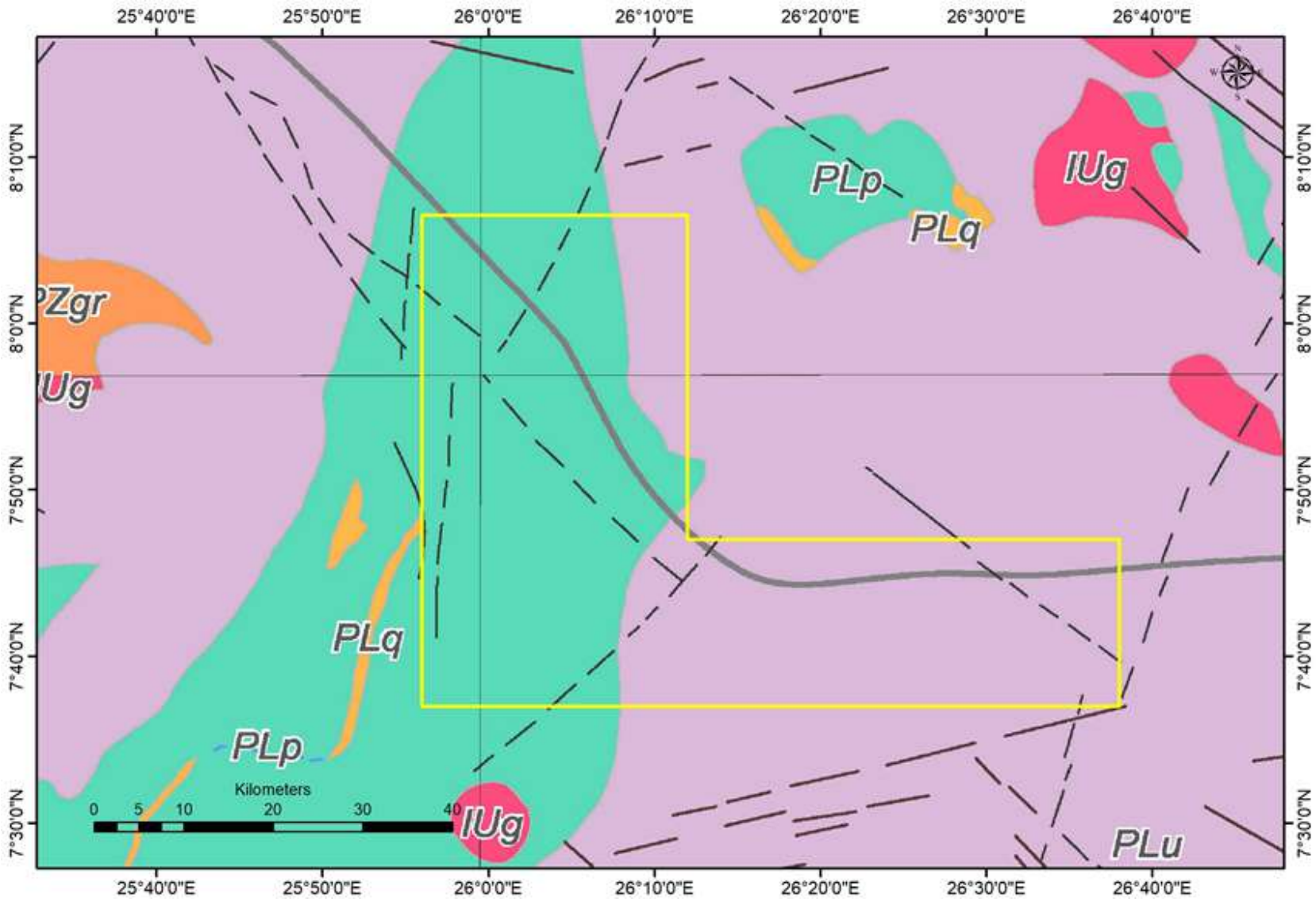

Fig. 10. Geological and structural maps of the study area (No details can be described at this level due to lack of field work)

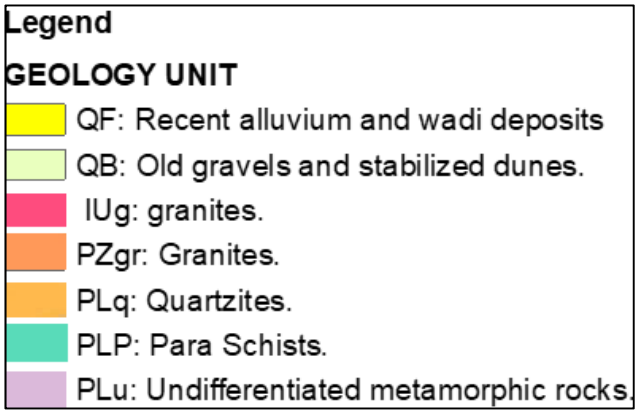

The lithological boundaries shown on the interpretation map are based on the interpretation of the image data. The unit descriptions and the ages of the relevant lithological units are very limited as they have been obtained from the legend of the existing maps and reports.

Essentially the ages and lithologies listed in Table (2) have been taken from the 1:2,000,000 scale geological map of the Republic of the Sudan published in 2004, this appears to be the most recent map published by GRAS (Geological Research Authority of Sudan) and it was one of the few maps available with a complete legend. The units and structures shown in the Northern Red Sea Hills area of this map appear to follow the Robertson Research International map which is based on the interpretation of Landsat hardcopy images.

4. REMOTE SENSING MINERAL PROSPECTING

The interpretation has been produced by careful study of the geomorphological expression of the surficial units in order to map the features relevant to exploration for alteration, VMS base metal sulphide deposits, quartz veins, iron ore and gold in the area of interest. A Landsat image which gives an overview of the area was studied at the outset to give the general structural framework and the features shown on the map were annotated directly on the digital image data in GIS (Table 4). This has been done by initially identifying and mapping small scale features such as foliation traces, so as to provide the evidence for larger structures. As a result, faults are shown where a displacement can be observed or inferred and the foliation provides the basis for understanding the regional structure. This process included a detailed first-pass annotation phase in which surface traces of fabrics, faults/fractures and lineaments, and some of the more obvious bedrock geological contacts were delineated. Cenozoic surficial cover boundaries and the remaining litho-unit contacts were inserted during a second pass.

The Landsat data proved very useful as it also covers the whole area and the colour composite image was helpful in discriminating the lithological units within the area, as similar data had been used for producing some of the published maps. However, the greater spatial resolution of the ASTER data was preferred for compiling detail on the lithostructural interpretation map.

The ASTER 7, 4, 2 band combination proved to be a great help in mapping structure, and the band ratio and PCA images pick out the lithological units. The main value of the ratio

images was in identifying alteration which might indicate mineralised zones, thus providing the basis for selecting the target areas.

To help guide interpretation, reference was made to the existing mapping, which was included with the data provided by COIPA Co., and various maps obtained from Al Neelain University. This information proved to be somewhat sketchy as the maps are generally small scale. In addition, some of the maps were provided without legends so the stratigraphic nomenclature/subdivisions, as well as information about the contained lithologies is very basic (see below). The interpretation was not extended beyond the permit boundaries in order to pick up features that may impact on the area, nevertheless structures and units which occur beyond the permit boundaries and impact on the area have been included in the interpretation. The large scale interpreted features have been examined in their regional context to check that they fit into the regional framework.

Table 4: GIS Layers Generated

GEOLOGY LAYERS	Comments
SRSH_Fabrics	Foliation traces derived from image interpretation, in this instance the fabric of the metamorphic rocks with variable trends mainly to the north & east.
SRSH_Geol_Boundaries	Geological boundaries derived from satellite image interpretation
SRSH_Dykes&Veins	Positive linear features interpreted as veins; linear features with dark tones interpreted as dykes; the composition is not known from interpretation
SRSH_Faults&Fractures	Faults fractures & linears derived from satellite image interpretation
SRSH_Geolunit_Polygons	Attributed layer of polygons for each geological unit with the relevant colour code
SRSH_Targets	Features identified for field investigation for the occurrence VMS sulphides & gold mineralisation.
SRSH_Minerals_BRGM	Location of mineral occurrences taken form BRGM geological map and other sources
FC_Drainage	The wadis, rivers and streams traced from the satellite image data and mapped directly into MapInfo.
DATA LAYERS	
COIBPA Block	Permit boundaries derived from coordinates provided & converted to MapInfo .tab files.
SRSH_Legend	Explanation of the features on the lithostructural interpretation maps.

An overall list of the layers generated during the compilation together with data layers used for reference is given in Table (4) and all layers have been compiled to the UTM projection (Zone 36N) and WGS84 datum.

The relevance of the geological features as interpreted is discussed below in section 3.2. All GIS layers generated for the interpretation are available for delivery to COIPA MINING CO., in PCI-Geomatica or an alternative GIS format if required.

4.1. Band Ratio Combination

In this band ratio Sabins's color composite image have produced after the analysis of the primary band ratios of 3/1 for iron oxide mapping, band ratio 5/7 for clay minerals and 3/5 for ferric oxides. The products are density sliced image for the band ratios 3/1 and 5/7 and color composite image which used in supervised classification (Fig. 11).

4.2. Matched Filtering

Matched Filtering maximizes the spectral response of a known endmember and suppresses the response of the composite unknown background, and then computes distribution of each endmember separately. This method does not, therefore, require knowledge of all the endmembers within the image. MF results are grey scale images with values from 0 to1, where 1 means perfect match (Adeli et al. 2008).

Two produced images (spectral reflectance of Kaolinite and spectral absorption pattern of iron oxide) in grey scale images with values from 0 to1, plus an average image of them were used to make a color composite image to enhance hydrothermal alteration zones in the area. For this purpose, Kaolinite distribution image, iron oxide distribution image made by MF method and average image were considered as a red, blue and green color respectively. In this image (Fig. 12) white pixels which are encircled by black ellipsoid.

4.3. Feature Oriented Principal Component Selection (FPCS)

Feature Oriented Principal Component Selection (FPCS) is a method of selection of some the image bands. By reducing input bands into PCA analysis, the chances of defining a unique PC for a specific mineral class will be increased. So, for an enhanced detection of alteration zones with respect to their indicative minerals, bands 1, 4, 5, 7 and bands 1, 3, 4, 5 are used to map hydroxyl and iron oxide minerals, respectively in Crosta method.

The false color composite image obtained using hydroxyl image (PC4 extracted from implementation of Crosta on Bands 1, 4, 5, and 7), iron oxide image (-PC4 extracted from implementation of Crosta on Bands 1, 3, 4, and 5) and average of these two images are depicted in red, blue and green, respectively. As it is observable in Figure (13), yellow pixels highlight hydrothermally altered area in study area.

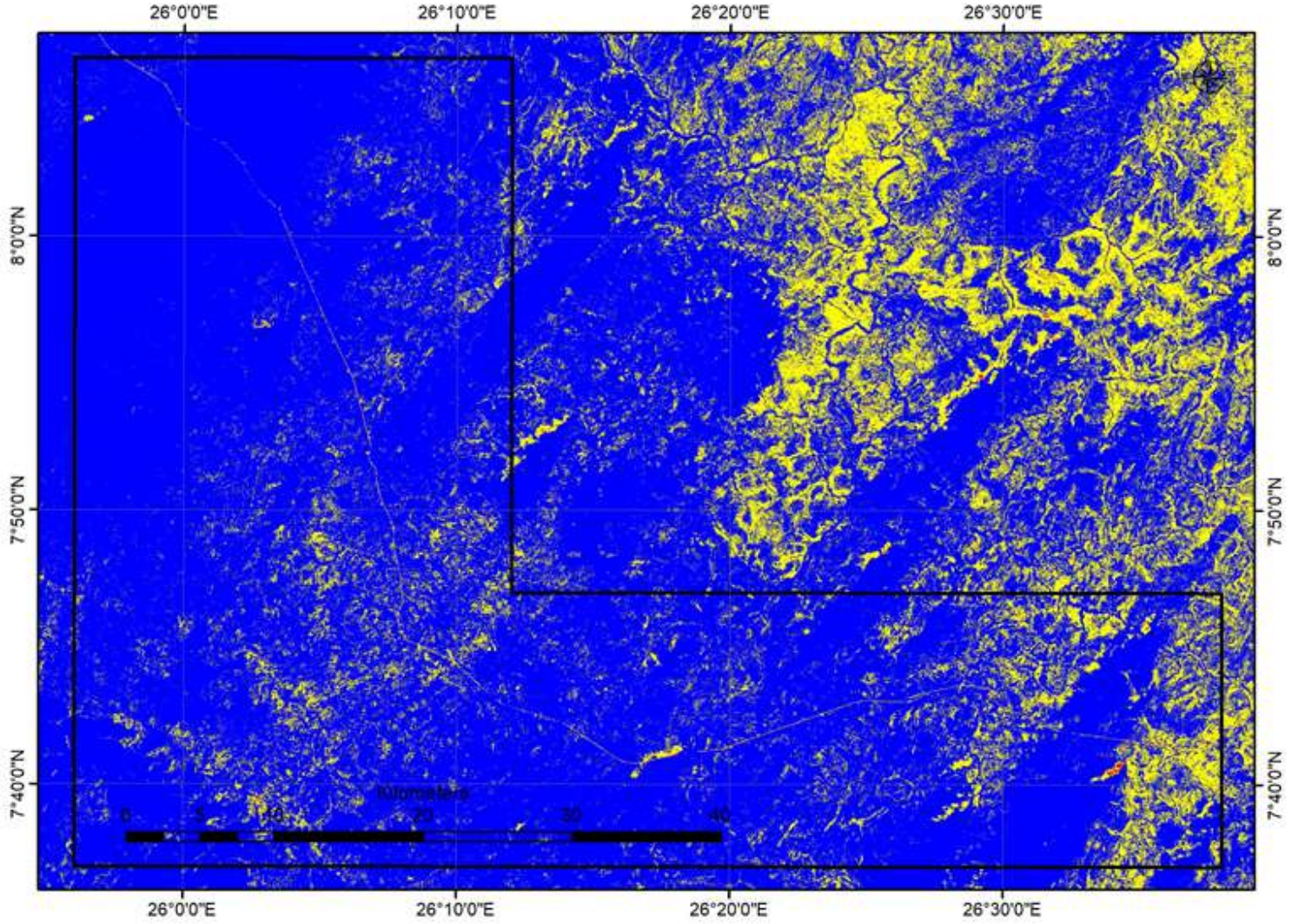

Fig. 11a1. Density sliced F-Image

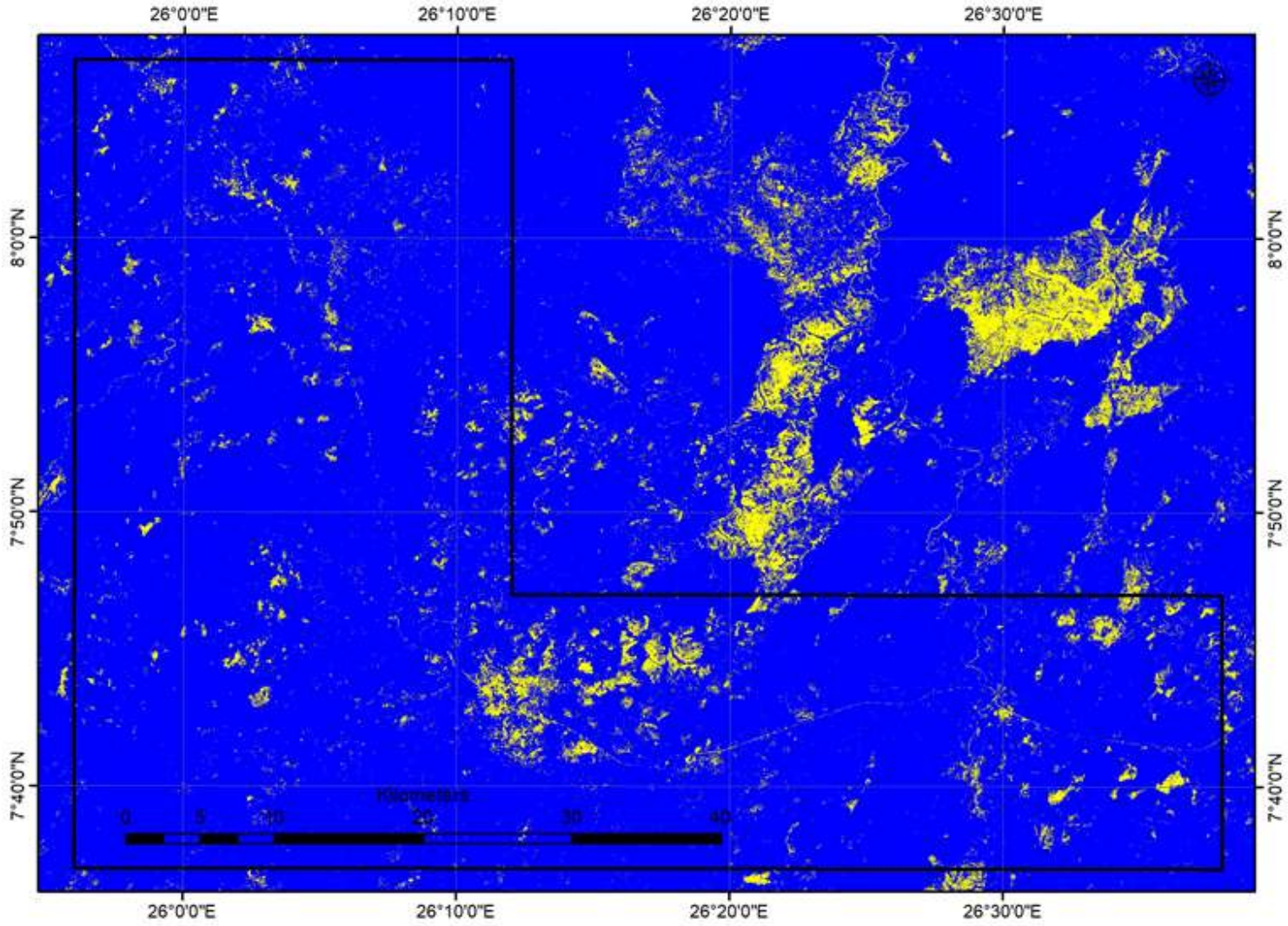

Fig. 11a2. Density sliced H-Image

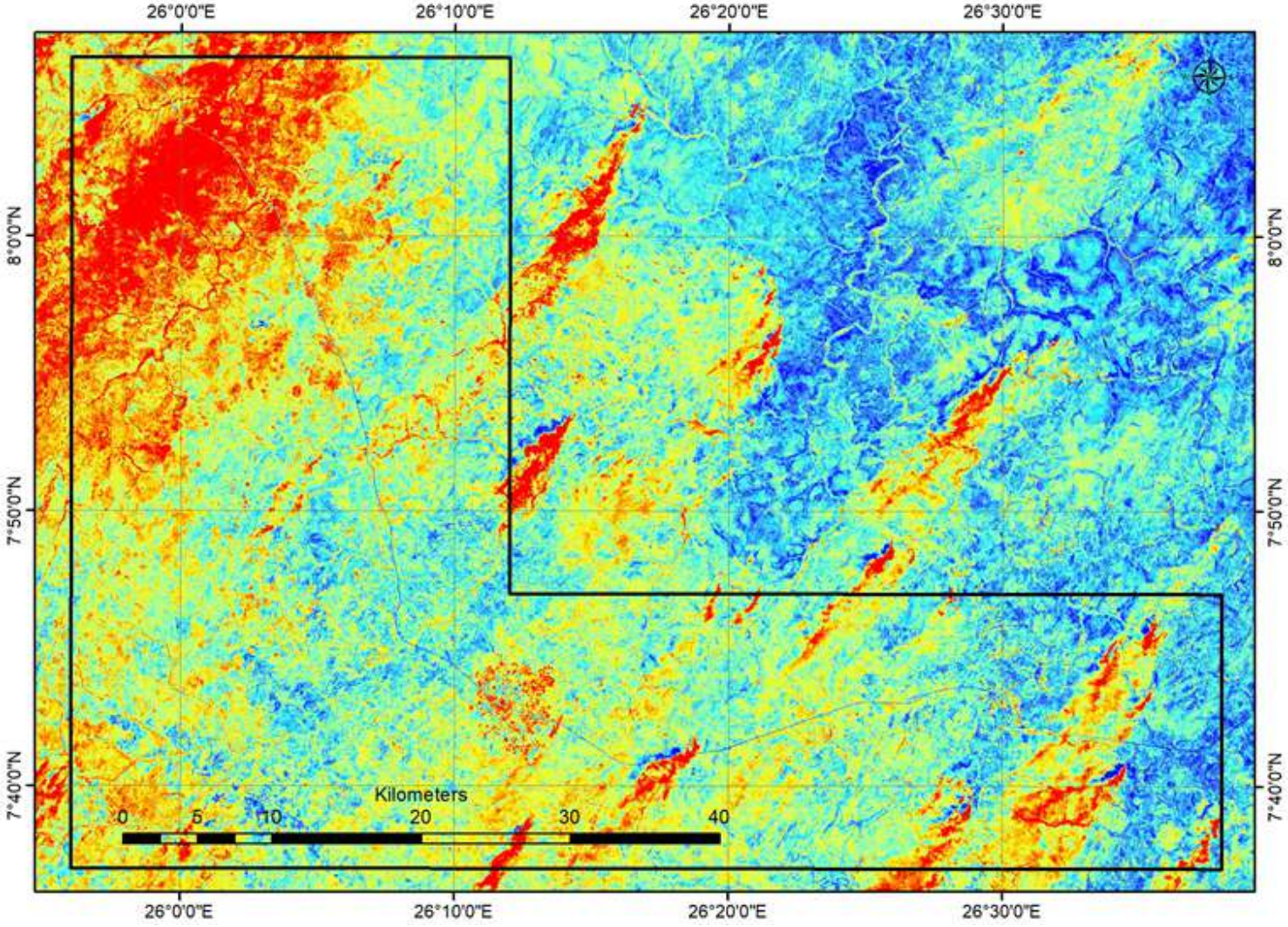

Fig. 11b1. F-Image

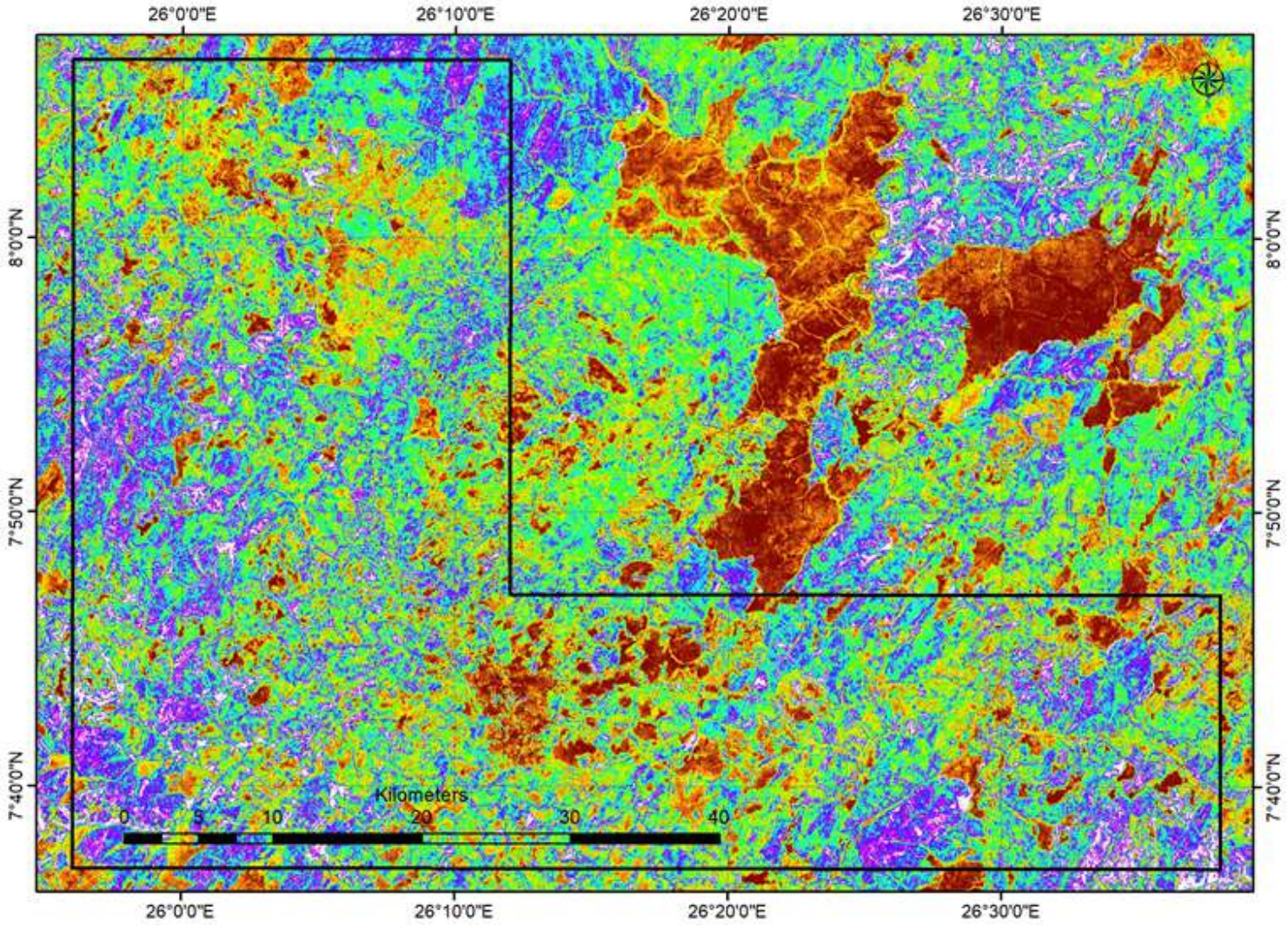

Fig. 11b2. H-Image

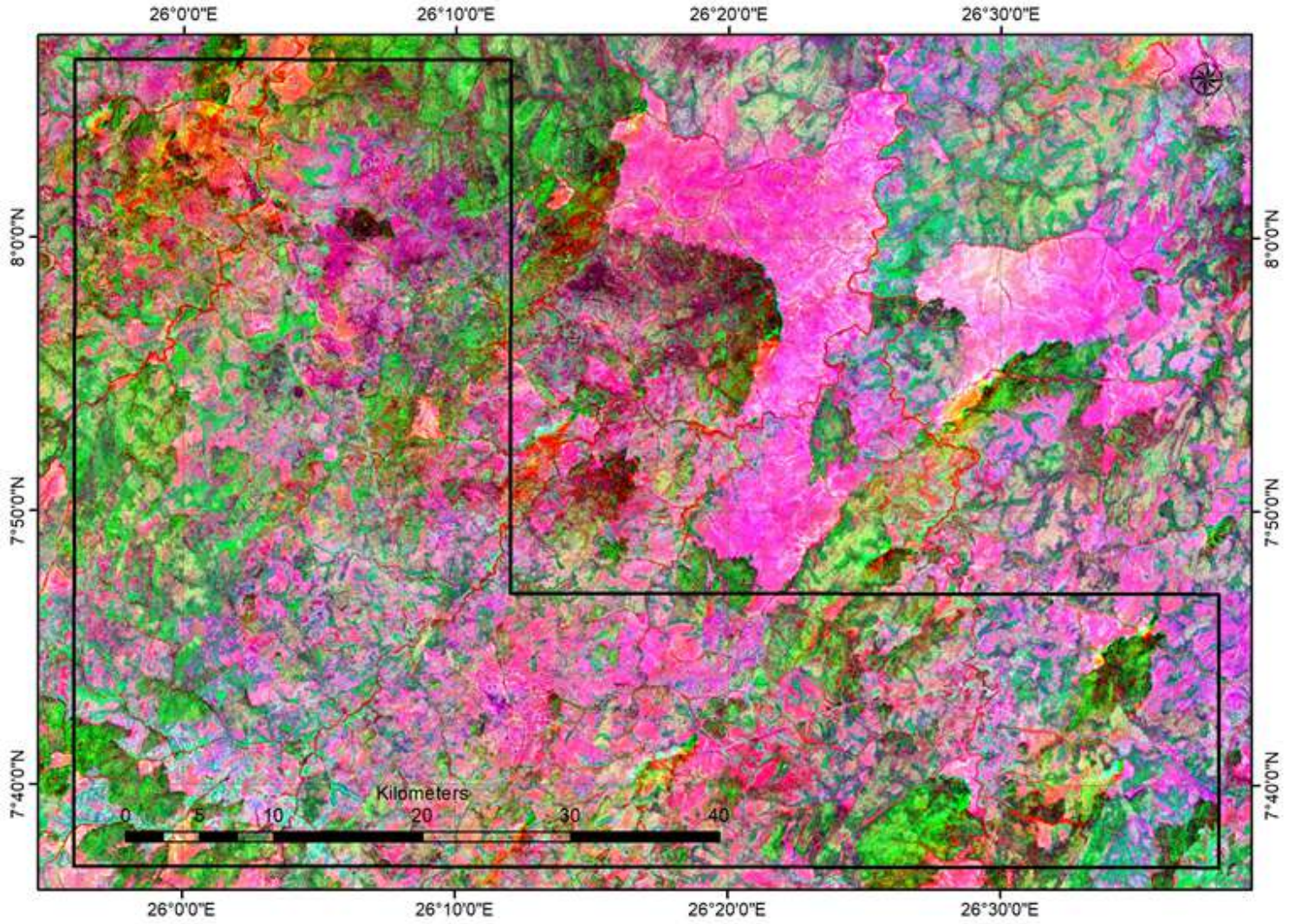

Fig. 12. Mineral composite image (Images utilized in the mineral prospecting work)

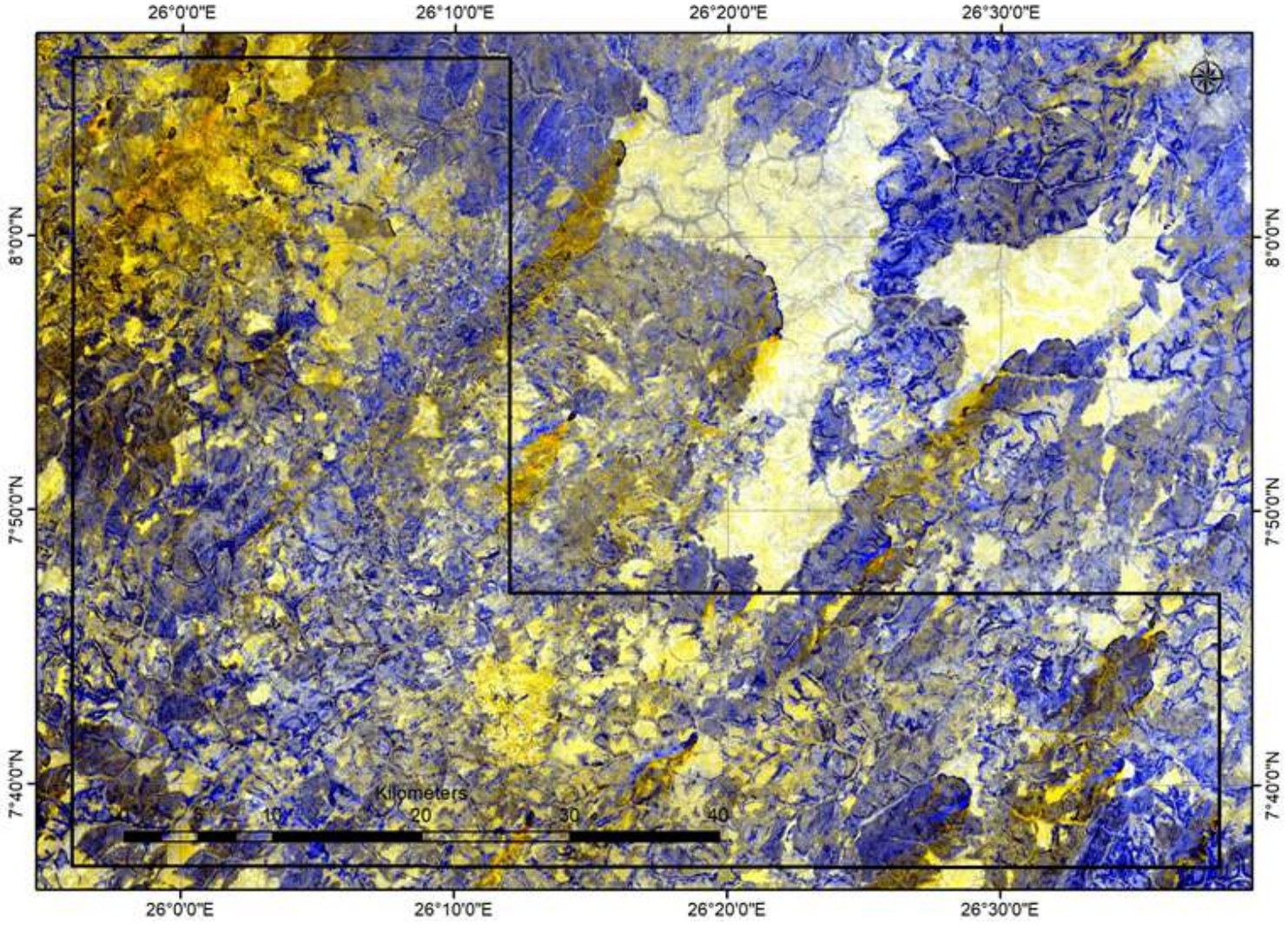

Fig. 13a. Crosta color composite image (Images utilized in the mineral prospecting work)

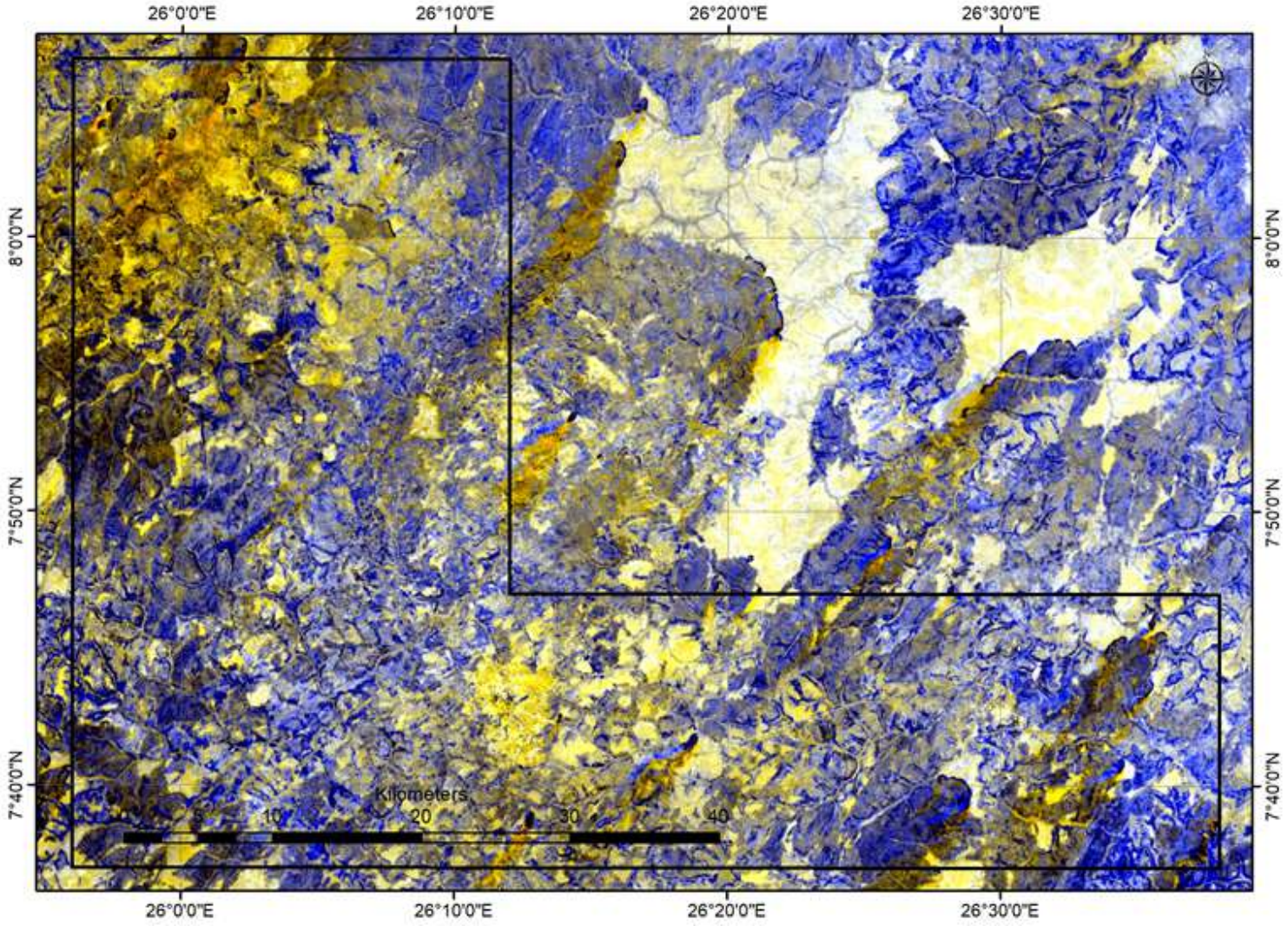

Fig. 13b. Crosta low pass filter image

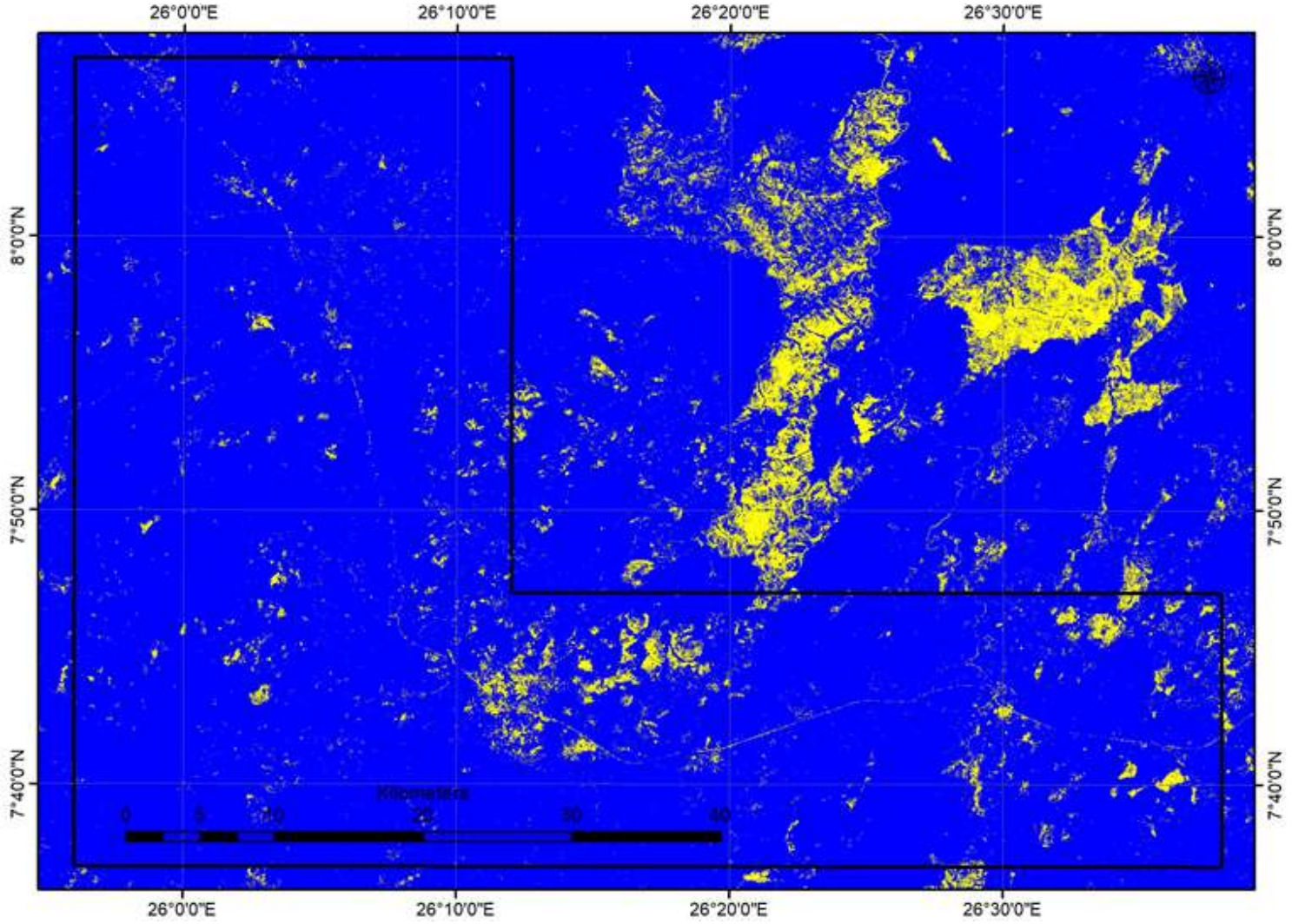

Fig. 13c. Crosta *Density Sliced Image*

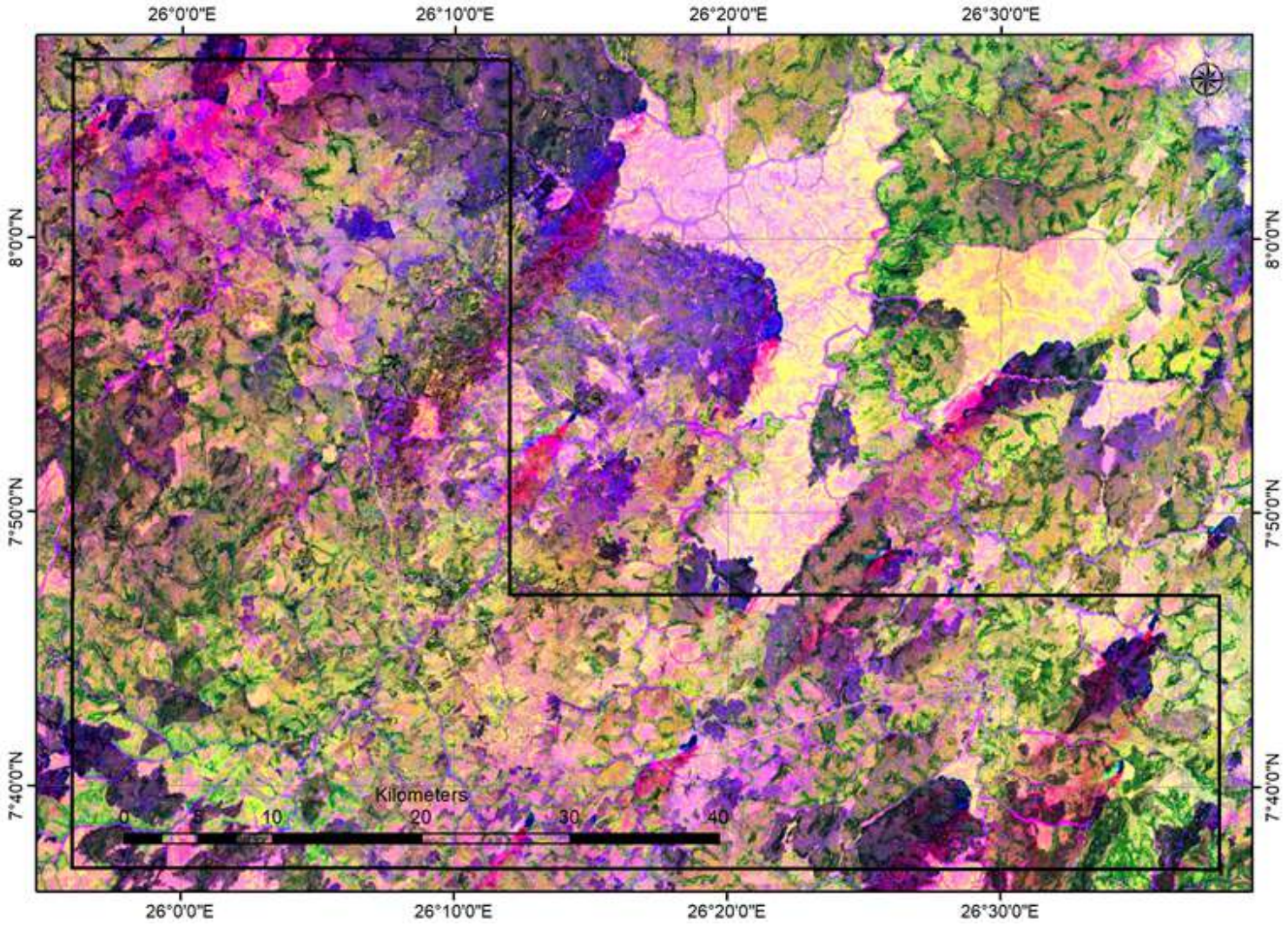

Fig. 14. Hydrothermal Color Composite Image

5. FINAL PRODUCT

The data review has confirmed that the gold and associated minerals Block EL 21 of the COIPA MINING concession area is underlain by extensions of the study area. The lithological unit present are considered to be similar to those areas of these belts that are known to host important base metal and gold mineralisation (Fig. 9).

The study area lies within a region known for gold occurrences and associated minerals. The mineralization is mainly structurally controlled. Most of the gold is found in quartz veins and their wall-rock alteration zones suggest that exploration is highly justified.

The satellite imagery interpretation of the concession areas has identified 5 target areas within the study area (Fig. 15), which is made up of 3 within southern part of Block and 2 within the northern part. These targets have been selected from alteration anomalies identified from the ratio images generated from the Landsat data during the processing stage (Smoky, Grey Quartz and pinkish white veins/Alteration/Host ratio & Advanced Argillic ratio), combined with geomorphic and structural features observed during the interpretation e.g. veins and small intrusive features. The parameters for the ratio images are given in Table (2). The targets have been checked against the original image data to avoid including spurious features which are sometimes produced by the processing.

The following figure (15) and Table (5) summarise the target areas identified in COIPA Block, the grid references are given as UTM Eastings/Northings Zone 36 to WGS84 datum. Where the target covers an irregular polygon the grid reference is taken at center of the polygon.

6. CONCLUSION AND RECOMMENDATION

I. The 6 promising targets revealed the enrichment of the area with alteration zones some of these zones are probable related to mineralization bodies, others could be related to other phenomena of masking and interference, careful field examination and sampling will have led to better filtered view for the whole area.
II. It is highly recommended to conduct fieldwork as soon as possible and updating the produced geological map.

Table 5: Potential mineralisation zones

Promising zones	**Area km²**
1	350
2	200
3	250
4	75
5	47

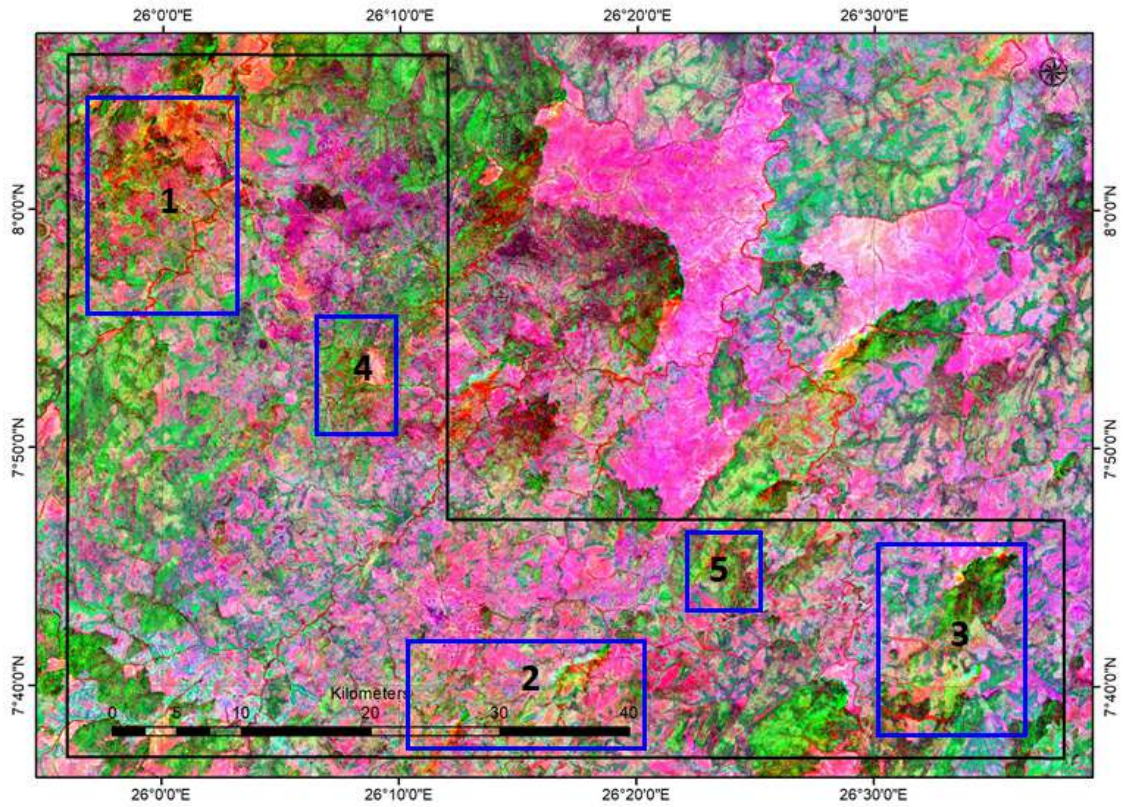

Fig. 15. Promising zones after located by remote sensing analysis

7. REFERENCE

Abdel Rahman, E. M., 1983. The geology of mafic-ultramafic masses and adjacent rocks south of the Ingessana igneous complex, Blue Nile Province, E. Sudan. Thesis, MSc., Portsmouth Polytechnic Univ.

Abdel Rahman, E. M., 1993. Geochemical and geotectonic controls of the metallogenic evolution of selected ophiolite complexes from the Sudan. PhD. Thesis University of Berlin, 175pp.

Abdel Magid, A. E. M., 1983. The geology of the metamorphic terrain around the south-west margin of the Ingessana Igneous complex, S. E. Sudan.

Unpubl. M. Phil. thesis, Portsmouth Polytechnic, England.

Adde, A. E. and Imam, A. A. 2005. Gold exploration in Qeissan area, southern Blue Nile State, S. E. Sudan.

Adde, et al. 2007. Gold exploration at Eyat concession, Qeissan area, S. E. Sudan.

Adde, A. E., Khalil, F.A. et al., 1993. Geology and gold mineralization, Qeissan area, Blue Nile Province, Sudan.

Afia, S. M. And Widatala, A., 1961. Investigation of the Hofrat El Nahas copper deposit. GMRD.

Almond, D. C., 1980. Structure and metamorphism of the basement complex of North – East Uganda. Overseas Geol. Miner. Resource, 10, pp. 146 – 163.

Bakhiet A. K., 1991. Geological and tectonic control of sulphide gold mineralization in Ariab Mineral District. Red Sea Hills, Sudan.

Civetta, L. De Vivo, B et al. 1980. Geological and structural outlines of the southern Sudan. Geodynamic Evolution of the Afro-Arabian Rift System. Roma, Accad. NazionaleDei Lincei.

De Vivo, B., Giunta, G. Et Al. 1980. Regional geochemical reconnissance on alluvial deposits in Southern Sudan. per. di miner. roma, 49 pp 23 - 43.

Dennen, W.H. & Norton, H.A. 1972. Geology and Geochemistry of Bauxite Deposits in Lower Amazon Basin. Econ. Geol. Vol. 72 Pp 82 – 89.

Gedeon, A.Z.; Butt, C.R.M. Et Al. 1977. The Application of Some Geochemical Analytical Techniques in Determining Total Composition of Some Lateritic Rocks. Jour. Geochem. Expl. Vol. 8, pp 283 - 303.

Gorden et al. 1972. Bauxite development in soil science. Amsterdam, Elsevier Pub. Co. 226p.

Goffe, J.S. 1949. Pedology, Second Edition. Pedology Publications. New Brunswick, New Jersy, USA.

Hunting Geology and Geophysics, 1980.Mineral Exploration in Juba area.

Idris, M.A. et al. 2002. Geology of The Bauxite Deposit of J. Twiga Area; Northwest, Sudan.

Ireland, A.W. 1948. Climate of the Sudan. Jour. Soil Science, London.

Kronberg, B.I. Couston, J.F. et al. 1979. Minor Element Geochemistry Of The Paragominas Bauxite, Brazil. Econ. Geol. & Bull of The Soc. Econ. Geol. Vol. 74 No 8 , pp 1869 - 1875.

Smirnov, V.I. 1962. Geology Of Mineral Deposit. Mir. Publishers; Moscow.

Tothill, J.D. 1948. A Note On The Origin Of The Soils Of The Sudan From The Point Of View Of The Man In The Field. J. Soil Sci. London.

Toum I. M. 1985.The Geology of the Qeissan area, Blur Nile Province, S. E. Sudan. M. Phil. Portsmouth Polytechnic, U.K.

El Rasheed, A. E. et al. 2004. Regional geological mapping and geochemical sampling of Qeissan-Kadalo District of southern Blue Nile State, Sudan.

Vail et al., 1986. Geology of southern Blue Nile province, Sudan. Bull. Geol. Res. Auth., Sudan, 37, pp., Sudan.

Vail et al., 1987. Late Proterozoic Tectonic Terranes in the Arabian – Nubian shield and their charachteristic mineralization. Geological Journal 22. Thiematic issue. 161- 174, John Wiley and Sons, Ltd..

Vail et al., 1988. Tectonic and evolution of proterozoic in north-east. African Journal, Journal of African earth Sciences. Vol. 1. No.3/4.

Vail J. R. 1983. The Arabian-Nubian shield, Proterozoic continental accretion.